

Universität
Rostock



Traditio et Innovatio



With the support of the
Erasmus+ Programme
of the European Union



Numerical Optimization Analysis of Cruise Vessels

Submitted on 31st August 2020

by

LUNGU Daniela-Laura | Erich-Schlesinger-Str. 19, Room 1.5.4.1 | 18059 Rostock |

danielalungu19@gmail.com

Student ID No.: 219 200 149

First Reviewer:

Prof. Dr. Eng./Hiroshima Univ. Patrick Kaeding
Pro-Rector of Studying, Teaching and Evaluation
Universitätsplatz 1, Room 124
18055 Rostock
Germany

Second Reviewer:

Dipl.-Ing. Stefan, Griesch
Senior Project Engineer
MV WERFTEN Wismar GmbH
18119 Rostock
Germany



Master Thesis

[This page is intentionally left blank]

Declaration of Authorship

I, *Daniela-Laura Lungu*, declare that this thesis and the work presented in it are my own and have been generated by me as the result of my own original research.

Where I have consulted the published work of others, this is always clearly attributed.

Where I have quoted from the work of others, the source is always given. With the exception of such quotations, this thesis is entirely my own work.

I have acknowledged all main sources of help.

Where the thesis is based on work done by myself jointly with others, I have made clear exactly what was done by others and what I have contributed myself.

This thesis contains no material that has been submitted previously, in whole or in part, for the award of any other academic degree or diploma.

I cede copyright of the thesis in favour of the University of Rostock.

Date:

31st of August, 2020

Signature:

A handwritten signature in black ink, appearing to read 'Lungu', written in a cursive style.

[This page is intentionally left blank]

ABSTRACT

One of the most important aspects to consider in ship design is the structural integrity for which yielding plays a decisive role. In order to have good strength in a ship, specially cruise vessels, which are large and complex structures, yield check is required to assure the safety under extreme loading conditions. To provide a good structure and maintain costs as limited as possible, structural optimization is carried out.

In this thesis, the main optimization methods are explained with emphasis on the two methods used for the strength analysis of the vessel. These are size (scantling) optimization and change of material and an optimization algorithm has been developed in order to implement these methods. They are assessed as two separate methods in the optimization process, implemented for one structural model, selected at the midship of a cruise vessel, between two transversal bulkheads, subjected to two independent loading conditions, sagging and hogging. The main objective of the optimization is to minimize production costs, whether it is by minimising the mass through thickness change of the panels, or by changing the material used to a material with better properties, such as higher strength allowance. For the validation of the optimization algorithm strength analysis has been carried out in ANSYS Academic Research Academic and CFD, version 18.2, with license provided by the University of Rostock.

The results obtained from the iterative process show that the two methods achieve structural optimization, but at different costs. The size optimization is a time-consuming method, and complicated to the extent that panel thicknesses have to be uniformly distributed for good weldability. On the other hand, the material change method is more practical from a shipyard point of view, since normal steel and high tensile steel have similar densities, providing almost similar mass, therefore, better structural strength with no need of considering thickness differences between panels. For both methods there are improvements to be considered for further analysis.

[This page is intentionally left blank]

TABLE OF CONTENTS

ABSTRACT.....	iv
TABLE OF CONTENTS	vi
List of Figures.....	viii
List of Tables	ix
List of Abbreviations and Symbols.....	ix
1 INTRODUCTION.....	1
1.1. Problem Formulation and Approach.....	1
1.2. Structure of the Thesis.....	2
2. THEORETICAL APPROACH IN STRUCTURAL OPTIMIZATION.....	4
2.1. FEM and FE Analysis in Mechanical Engineering.....	4
2.1.1. FEM Procedure.....	4
2.1.2. Equilibrium Equations	5
2.1.3. Strain-Displacement Relations.....	6
2.1.4. Stress – strain constitutive equations.....	7
2.1.5. Boundary conditions	8
2.2. General Aspects of Structural Optimization.....	8
2.3. Types of Optimization	9
2.3.1. Topology Optimization.....	10
2.3.2. Shape Optimization.....	11
2.3.3. Material Optimization (Change of material grade).....	14
2.4. The Objective of the Optimization Process	14
2.5. Constraints.....	15
2.5.1. Technological Constraints	15
2.5.2. Geometrical Constraints	16
2.5.3. Structural Constraints	16
2.6. Design Variables.....	19
2.7. Steel Properties and Behaviour	20
2.7.1. Linear Elastic Material Condition	20
2.7.2. Yield Criteria.....	21
2.8. Load Condition.....	23
2.8.1. Sagging	24
2.8.2. Hogging	25
3. NUMERICAL MODEL	27

3.1.	ANSYS Parametric Design Language (APDL)	28
3.2	Sample Model Description	29
3.2.1	Boundary Conditions and loads	30
3.3	Main Model Description	30
3.3.1	Boundary Conditions and Loads	33
3.4	Algorithm Development	35
4.	NUMERICAL OPTIMIZATION ANALYSIS	37
4.1	Change in Plate Thickness	37
4.1.1	Sagging	38
4.2	Change in Material (Steel) Grade	47
4.3	Results	52
4.3.1	Sagging	53
4.3.2	Hogging	56
5	CONCLUSION	60
6	FURTHER WORK	63
7	ACKNOWLEDGMENTS	64
8	REFERENCES	65
	APPENDIX A - Results of size optimization – Sagging loading condition	68

List of Figures

Figure 1 Stress states in an infinitesimal element of a two-dimensional elastic body (Stolarski, Nakasone, & Yoshimoto, 2006).....	6
Figure 2 Topology Optimization (Bendsoe & Sigmund, 2003).....	10
Figure 3 Shape Optimization (Bendsoe & Sigmund, 2003) Size Optimization	11
Figure 4 Size/Scantling Optimization of a Truss Structure (Bendsoe & Sigmund, 2003).....	12
Figure 5 Sagging Bending Moment (Menon, 2020).....	25
Figure 6 Hogging Bending Moment (Menon, 2020).....	25
Figure 7 Sign Convention for Shear Forces and Bending Moments (DNV-GL, 2017).....	26
Figure 8 Sample model structure and stiffened panels in the structure.....	29
Figure 9 Boundary conditions and reactions on the sample model.....	30
Figure 10 FEM Model of Main Structure – Cruise Vessel (MV WERFTEN Wismar, n.d.).....	31
Figure 11 Section of the vessel considered for structural optimization.....	32
Figure 12 Stiffened plate structure (Paik & Kim, 2002).....	33
Figure 13 Coupled boundary conditions and loads acting on the ship.....	34
Figure 14 Boundary conditions and loads acting on the selected structure.....	34
Figure 15 Optimization Algorithm.....	35
Figure 16 Comparison between structure at initial condition and section with changed thickness to 4mm.....	37
Figure 17 Section ID of thickness 4mm.....	38
Figure 18 Comparison between initial structure and structure after the first iteration.....	40
Figure 19 Comparison between first and second iteration.....	41
Figure 20 Comparison between second and third iteration.....	42
Figure 21 Comparison between third and fourth iteration.....	43
Figure 22 Comparison between fourth and fifth iteration.....	44
Figure 23 Comparison between fifth and sixth (last) iteration.....	46
Figure 24 Plot of usage of the panels. Left - Initial case and right - structure at 4mm thickness.....	48
Figure 25 Usage factor distribution after the material change.....	50
Figure 26 Plot of usage of the panels during hogging loading case. Left - Initial case and right - structure at 4mm thickness.....	51
Figure 27 Usage factor distribution after the material change.....	52
Figure 28 Nodal stress assessment - Initial case.....	53
Figure 29 Nodal stress assessment - structure at 4mm thickness.....	53
Figure 30 Nodal stress assessment - Optimized structure.....	53
Figure 31 Elemental stress distribution of optimized structure - Sagging.....	54
Figure 32 Zoom over Figure 31.....	54
Figure 33 Optimization loop for the sagging loading condition.....	55
Figure 34 Mass behaviour proportional to the size optimization.....	55
Figure 35 Cost estimation of the structure after size optimization.....	55
Figure 36 Cost Increase for Material Change – Sagging.....	56
Figure 37 Optimization loop for the hogging loading condition.....	57
Figure 38 Mass behaviour with respect to size optimization.....	58
Figure 39 Cost estimation of the structure after size optimization.....	58
Figure 40 Cost Increase for Material Change - Hogging.....	58

List of Tables

Table 1 Weakening of the structure - Uniform thickness of 4mm.....	39
Table 2 Difference in [%] of stresses between initial case and structure at 4mm.....	39
Table 3 Difference in [%] of the stress values in panels.....	40
Table 4 Difference in [%] of stress in panels after the second iteration	41
Table 5 Difference in [%] of stress in panels after the third iteration.....	42
Table 6 Difference in [%] of stress in panels after the fourth iteration.....	43
Table 7 Difference in [%] of stress in panels after the fifth iteration.....	44
Table 8 Sixth iteration - change in thickness - Sagging.....	45
Table 9 Difference in [%] of stress in panels after the sixth iteration.....	46
Table 10 Usage factor of panels for the initial case and the structure at 4mm thickness – Sagging bending moment.....	48
Table 11 Usage factors and new material ID after the material change – Sagging	49
Table 12 Usage factor of panels for the initial case and the structure at 4mm thickness - Hogging	51
Table 13 Usage factors and new material ID after the material change - Hogging	52
Table 14 First Iteration – size optimization	68
Table 15 Second Iteration - size optimization	68
Table 16 Third Iteration - size optimization	68
Table 17 Fourth Iteration - size optimization.....	69
Table 18 Fifth Iteration - size optimization	69
Table 19 Sixth Iteration - size optimization.....	69

List of Abbreviations and Symbols

APDL – Ansys Parametric Design Language

FEM – Finite Element Method

DNV – Det Norske Veritas

GL – Germanischer Lloyd

[This page is intentionally left blank]

1 INTRODUCTION

1.1. Problem Formulation and Approach

This thesis describes the optimization techniques necessary to improve the structure of a cruise vessel. As described by the Telegraph (Kim, 2018), “A cruise ship’s structural grid features a series of webs, starting at the hull and coming up through beams throughout the ship. Every fourth web or so is supported by a huge sheet of steel”. In shipbuilding, the construction of a cruise vessel is a big challenge as many aspects have to be considered in detail from the initial design until the welding of the plates. And this is again confirmed in the same paper mentioned above by (Kim, 2018) as “Cruise ships are like giant floating tubes. Unlike buildings on land, the majority of the walls are actually part of the ship’s structure. Cutting holes through this giant tube in the process of building different parts of the ship can make the whole structure weak.”. To make sure the vessel is a safe home for the approximately 9500 passengers on board (MV WERFTEN Wismar, n.d.) while on their vacation, structural safety has to be ensured and by over-stiffening the structure the weight will increase, bringing extra operational costs overall.

In this paper, ship structural optimization methods will be introduced and explained, along with its importance in the initial design of a vessel. The designer must consider stress analysis, material behaviour and failure methods during the design process, keeping good structural integrity (Introduction to structural integrity, n.d.). First, good stress distribution in the structural members of a ship provides a longer lifespan of the ship and more chances of survival in different sea states, preventing failures such as yielding in zones subjected to high stress. Second, the deadweight is a factor that defines the capability of a ship to transport, respectively its ability to carry more goods on-board, or respectively to cruise vessels, more passengers, more resources or the possibility of increasing the loads on certain sections of the structure. Therefore, to increase the deadweight of a ship, the total lightweight must be reduced to a point of validation of the efficiency of the structural optimization and definition of the reduction in construction costs.

According to (Sekulski, 2009) structural optimization can be expressed as finding the optimum for the objective function subject to design constraints, defined via three main methods: topology optimization, shape optimization, size (scantling) optimization. A fourth criterion is also considered, material optimization, that introduces the possibility of changing the material

grade within the optimization process according to the experience and capabilities of a shipyard.

The problem of structural optimization is complex if to consider all four methods in one algorithm, therefore in this thesis, the emphasis is on size optimization (scantling optimization), by modifying the thickness of the plates in the structure and material optimization, with the main objective on reducing the lightweight of a cruise vessel and its production costs confirmed by performing a basic cost estimation. For both types of structural optimization, the topology and shape are fixed (Sekulski, 2009).

As mentioned in the first part of the problem formulation, structural optimization is of great importance for the very beginning of the initial design and calculation for a ship structural strength, therefore precision must be achieved in stress and displacement computation and for this Finite Element Method (FEM) is used for the strength analysis of the structure. In the development of the thesis, the ANSYS Mechanical APDL Software has been used for performing strength simulations on the model through the implementation of macros (codes) written in Ansys Parametric Design Language.

1.2. Structure of the Thesis

The division of the thesis is done as follows:

Chapter 2 – This chapter offers a theoretical approach over what structural optimization means and what are the methods most commonly used and which method is used for this project. Also, it provides a sense of what the objective, constraints and design variables of the structural optimization are; and lastly, the theoretical explanation of the material used in shipbuilding and the criteria needed for the strength analysis are explained to clarify what are the limitations faced during the implementation of the optimization algorithm.

Chapter 3 – The chapter provides an overview of the description of the sample model used to implement the optimization algorithm and the description of the main model subject to structural optimization in this project. Lastly, the detailed explanation of the developed algorithm is provided.

Chapter 4 – Here the results of the structural optimization techniques used are included, along with a brief discussion over the results from the two considered loading cases, sagging and hogging.

Chapter 5 – A conclusion is presented with a subjective note, over the entire work detailed in the thesis.

Chapter 6 – gives a perspective over the future works that can be accomplished in making the optimization process more accurate.

2. THEORETICAL APPROACH IN STRUCTURAL OPTIMIZATION

2.1. FEM and FE Analysis in Mechanical Engineering

The Finite Element Method (FEM) is explained by (Stolarski, Nakasone, & Yoshimoto, 2006) as a mathematical technique used for solving systems of partial differential (or integral) equations. The FEM is formulated using two main methods: one based on the direct variational method – e.g. Rayleigh-Ritz method – and one based on the weighted residuals method – e.g. Galerkin's method.

On a more practical approach towards numerical analysis using FEM, (Thompson & Thompson, 2017) explain that in engineering, FEM is used to divide a system of whose behaviour cannot be predicted through closed-form equations into small pieces, called elements, whose solution can be approximated. An important aspect of this method is that the geometry is defined by points in space called nodes. Each node has a set of degrees of freedom (temperature, displacement, etc.), varying depending on the type of analysis. Each node is attached to an element, some being shared by more elements, depending on the element type used and they define the mathematical interactions of the degrees of freedom (DOFs). In complex structures where there exist continuum elements, the interaction among the DOFs is estimated by numerical integration over the element and all the individual elements are united to form a set of equations representing the system to be analyzed.

Just as a regular polygon approaches a perfect circle as the number of sides approaches infinity, a finite element model approaches a perfect representation of the system as the number of elements becomes infinite. This introduces the size of elements used in numerical analysis, where the smaller the element defined, the more accurate the results, but this comes with a cost increase in terms of computation time and manpower assigned to interpret the results, still being a faster method than manually calculating all the individual equations of each system. The benefit from this method lies in the ability to solve arbitrarily complex problems for which analytical solutions are not available or would be too expensive to solve by hand (Thompson & Thompson, 2017).

2.1.1. FEM Procedure

Limited to static elasticity problems, where there is no time variation, the Finite Element Method has been developed as one of the powerful numerical methods to obtain approximate

solutions for various kinds of elasticity problems and can be better described in the following steps (Stolarski, Nakasone, & Yoshimoto, 2006, p. 15):

- **Procedure 1:** *Discretization* - Divide the object of analysis into a finite number of finite elements.
- **Procedure 2:** *Selection of the interpolation function* - Select the element type or the interpolation function which approximates displacements and strains in each finite element.
- **Procedure 3:** *Derivation of element stiffness matrices* - Determine the element stiffness matrix which relates forces and displacements in each element.
- **Procedure 4:** *Assembly of stiffness matrices into the global stiffness matrix* - Assemble the element stiffness matrices into the global stiffness matrix which relates forces and displacements in the whole elastic body to be analyzed.
- **Procedure 5:** *Rearrangement of the global stiffness matrix* - Substitute prescribed applied forces (mechanical boundary conditions) and displacements (geometrical boundary conditions) into the global stiffness matrix, and rearrange the matrix by collecting unknown variables for forces and displacements, say in the left-hand side, and known values of the forces and displacements in the right-hand side to set up simultaneous equations.
- **Procedure 6:** *Derivation of unknown forces and displacements* - Solve the simultaneous equations set up in Procedure 5 above to solve the unknown variables for forces and displacements. The solutions for unknown forces are reaction forces and those for unknown displacements are deformations of the elastic body of interest for given geometrical and mechanical boundary conditions, respectively.
- **Procedure 7:** *Computation of strains and stresses* - Compute the strains and stresses from the displacements obtained in Procedure 6 by using the strain–displacement relations and the stress-strain relations explained later.

2.1.2. Equilibrium Equations

Considering the static equilibrium state of a small rectangle (element), see below Figure 1 with its sides parallel to the coordinate axes in a two-dimensional elastic body, with body forces F_x and F_y acting in the direction of x - and y - axes, the equations of equilibrium in the elastic body can be derived as follows (Stolarski, Nakasone, & Yoshimoto, 2006):

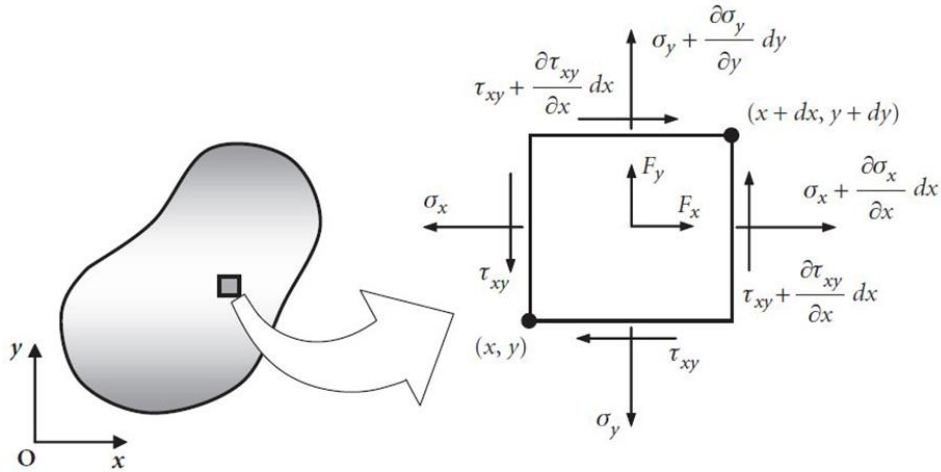


Figure 1 Stress states in an infinitesimal element of a two-dimensional elastic body (Stolarski, Nakasone, & Yoshimoto, 2006)

$$\begin{cases} \frac{\partial \sigma_x}{\partial x} + \frac{\partial \tau_{xy}}{\partial y} + F_x = 0 \\ \frac{\partial \tau_{yx}}{\partial x} + \frac{\partial \sigma_y}{\partial y} + F_y = 0 \end{cases} \quad (1)$$

where σ_x and σ_y – normal stresses in the x- and y-axes, and τ_{xy} and τ_{yx} shear stresses acting in the x-y plane. The shear stresses τ_{xy} and τ_{yx} are generally equal to each other due to the rotational equilibrium of the two-dimensional elastic body around its centre of gravity (Stolarski, Nakasone, & Yoshimoto, 2006).

2.1.3. Strain-Displacement Relations

Regarding the strain-displacement relations, (Stolarski, Nakasone, & Yoshimoto, 2006) explains that if the deformation of a two-dimensional elastic body is infinitesimally small under the applied load, the normal strains ε_x and ε_y are expressed by the following equations:

$$\begin{cases} \varepsilon_x = \frac{\partial u}{\partial x} \\ \varepsilon_y = \frac{\partial v}{\partial y} \\ \gamma_{xy} = \frac{\partial v}{\partial x} + \frac{\partial u}{\partial y} \end{cases} \quad (2)$$

where u and v are infinitesimal displacements in the directions of the x and y- axes.

2.1.4. Stress – strain constitutive equations

The stress–strain relations describe states of deformation, strains induced by the internal forces, or stresses resisting against applied loads. These relations depend on the properties of the material, and they are determined experimentally and often called constitutive relations or constitutive equations (Stolarski, Nakasone, & Yoshimoto, 2006).

In the two-dimensional elasticity theory, the three-dimensional Hooke's law which is an example of the constitutive equation is converted into two-dimensional form by using the plane stress approximation (for thin plates) and the plain strain approximation (when plate thickness in the z-axis is large).

In this work, since we utilised the shell elements (thin plates), the plane stress approximation will be described. For thin plates, for example, one can assume the plane stress approximation that all the stress components in the direction perpendicular to the plate surface vanish, that is, $\sigma_z = \tau_{zx} = \tau_{yz} = 0$. The stress–strain relations in this approximation are written by the following two-dimensional Hooke's law:

$$\begin{cases} \sigma_x = \frac{E}{1-\nu^2}(\varepsilon_x + \nu\varepsilon_y) \\ \sigma_y = \frac{E}{1-\nu^2}(\varepsilon_y + \nu\varepsilon_x) \\ \tau_{xy} = G\gamma_{xy} = \frac{E}{2(1+\nu)}\gamma_{xy} \end{cases} \quad (3)$$

or

$$\begin{cases} \varepsilon_x = \frac{1}{E}(\sigma_x - \nu\sigma_y) \\ \varepsilon_y = \frac{1}{E}(\sigma_y - \nu\sigma_x) \\ \gamma_{xy} = \frac{\tau_{xy}}{G} = \frac{2(1+\nu)}{E}\tau_{xy} \end{cases} \quad (4)$$

The normal strain component ε_z in the thickness direction, however, is not zero, but $\varepsilon_z = -\nu(\sigma_x + \sigma_y)/E$. The plane stress approximation satisfies the equations of equilibrium, nevertheless, the normal strain in the direction of the z-axis ε_z must take a special form, that is, it must be a linear function of coordinate variables x and y in order to satisfy the compatibility condition which ensures the continuity conditions of strains. Since this approximation imposes a special requirement for the form of the strain ε_z and thus the forms of the normal stresses σ_x and σ_y , this approximation cannot be considered as a general rule.

Strictly speaking, the plane stress state does not exist in reality (Stolarski, Nakasone, & Yoshimoto, 2006).

2.1.5. Boundary conditions

When solving the partial differential equation (equilibrium equation), there remains indefiniteness in the form of integral constants. To eliminate this indefiniteness, prescribed conditions on stress and/or displacements must be imposed on the bounding surface of the elastic body. These conditions are called boundary conditions. There are two types of boundary conditions: mechanical boundary conditions prescribing stresses or surface tractions and geometrical boundary conditions prescribing displacements (Stolarski, Nakasone, & Yoshimoto, 2006).

2.2. General Aspects of Structural Optimization

In optimization of a design, the design objective could be simply to minimize the cost of production or to maximize the efficiency of production, which is to minimize the total weight of the structure with consideration to constraints on geometry, stress and displacement in the structure under the design loads (Svanberg, n.d.). To implement the optimization of the structure, an objective function is used as a function of the design and state variables, which are the parameters to be changed in the optimization process. Other important criteria to consider are the constraints which are linear or nonlinear functions, explicit or implicit of the design variables (Rigo & Rizzuto, 2003).

In the recent years, development of technology has reached peaks in the domain of mechanical engineering and structural optimization plays an important role in the whole process as optimization methods have been integrated into softwares to ease the achievement of more accurate results in the Finite Element Analysis of engineering structures, reducing considerably the weight of structural members and the costs of production, keeping or improving the structural integrity (Haftka & Sobieszczanski-Sobieski, 2009).

The computerized analysis of structures, via models that discretize the structure into many finite elements, has become popular in the 1960s through numerical optimization started by L. Schmit (Haftka & Sobieszczanski-Sobieski, 2009).

Structural optimization is a complex area of study and (Bendsoe & Sigmund, 2003) describe it as the domain that combines mechanics, variational calculus, and mathematical programming to obtain better designs of structures.

In the present case, the optimization problem is subject only to stress limit constraints and deflection of structure, therefore, each part of the structure is stressed to its limit, imposed by material properties, under at least one loading condition, sagging or hogging being the main extreme wave bending moments considered for marine structures (Haftka & Sobieszczanski-Sobieski, 2009). The stress constraint implies that the structure will be limited by yielding (see Section 2.7.2) strength values assessed by considering a partial safety factor calculated based on DNV (DNV-GL, 2015) rules. The displacement of the structure is also kept in mind along with stress variation in the structure.

In the industry of shipbuilding, structural optimization represents a challenge, especially in the global structural optimization of a vessel. (Hughes, 1998, p. 71) mentions that for a structure such as the hull of a vessel that requires optimization there are typically 100 to 200 design variables, involving high computational costs even with sequential linear programming methods. To be able to solve the optimization problem of a complex structure, (Hughes, 1998, p. 71) introduces the concept of *submodules*, which represent “a region of structure in which a sufficient number of scantlings are linked, either by fixed structural geometry or by explicit constraints linking two or more scantlings, such that the structure forms a logical entity from an optimization point of view.” (Hughes, 1998).

2.3. Types of Optimization

Mentioned briefly in the introduction are the main methods that are used in structural optimization and (Sekulski, 2009) defines them as: topology optimization (main focus on weight optimization) by modifying the distribution of the material in the structure, respectively modifying the topological properties; shape optimization identifies the optimum structural shape in compliance with the initial constraints; and size optimization (scantling optimization) responsible with changing the dimensions of structural members such as plate thickness, longitudinal and transversal stiffening members and the spacing between longitudinal and transversal structural elements. A fourth criterion is also considered, material optimization as mentioned by (Sekulski, 2009), introducing the possibility of changing the material grade within the optimization process according to the experience and capabilities of a shipyard.

2.3.1. Topology Optimization

Topology optimization of solid structures involves the determination of features such as the number and location and shape of holes and the connectivity of the domain. The purpose of topology optimization is to find the optimal layout of a structure within a specified region. The only known quantities in the problem are the applied loads, the possible support conditions, the volume of the structure to be constructed and possibly some additional design restrictions such as the location and size of prescribed holes or solid areas. In this problem the physical size and the shape and connectivity of the structure are unknown.

In the design of the topology of a structure, it is of interest the determination of the optimal placement of a given isotropic material in space, i.e., determining which points of space should be material points and which points should remain void (no material) (Bendsoe & Sigmund, 2003).

In aerospace and automobile industry topology optimization has proven to be most efficient in weight minimization, unlike the shipbuilding industry where the majority of the lightship weight is comprised of continuous panels that form the hull shape and the internal main structural members such as decks or transversal and longitudinal bulkheads, that cannot be optimized using topology optimization due to the necessity of keeping the hull watertight and providing water and weather-tight compartments inside the ship to maintain the integrity and safety of the structure.

In Figure 2 below, the topology optimization is represented by (Bendsoe & Sigmund, 2003) in their book through a structure like a black and white rendering, in a fixed design domain. On the left is the initial structure and on the right is the optimized structure. We can observe that this method is not suitable for large panels optimization in ship design.

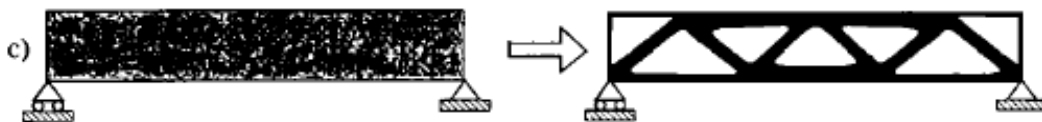


Figure 2 Topology Optimization (Bendsoe & Sigmund, 2003)

2.3.2. *Shape Optimization*

In its most general setting, shape optimization of continuum structures should consist of a determination for every point in space if there is material in that point or not. Alternatively, for a FEM discretization, every element is a potential void or structural member (Bendsoe & Sigmund, 2003).

(Lindemann & Kaeding, 2010) mention in their paper that shape optimization is the method that changes the geometry of a structure while maintaining topology. As mentioned previously, the optimization method most suitable for this project cannot be shape optimization as one of the two main constraints for this project is the geometry of the structure, which has to remain as fixed constraint, giving no opportunity for shape optimization of the cruise vessel.

This matter can be observed in the behaviour of the mechanical structure subject to shape optimization as described in Figure 3 below, by (Bendsoe & Sigmund, 2003), where the weight has been reduced by deleting material which does not play a critical role for the integrity of the structure.



Figure 3 Shape Optimization (Bendsoe & Sigmund, 2003) **Size Optimization**

(Bendsoe & Sigmund, 2003) describe the typical sizing problem, where the goal may be to find the optimal thickness distribution of a linearly elastic plate or the optimal member areas in a truss structure. The optimal thickness distribution minimizes (or maximizes) a physical quantity such as the mean compliance (external work), peak stress, deflection, etc. while equilibrium and other constraints on the state and design variables are satisfied.

In their book, (Bendsoe & Sigmund, 2003) also mention that the design variable is the thickness of the plate and the state variable may be its deflection or stress values. The main feature of the sizing problem is that the domain of the design model and state variables is known a priori and is fixed throughout the optimization process. This method is optimal for weight reduction in the shipbuilding industry. In Figure 4, an illustration from (Bendsoe & Sigmund, 2003) shows

how the scantling/size optimization changes the thickness of the truss analysed, by maintaining the initial geometry.

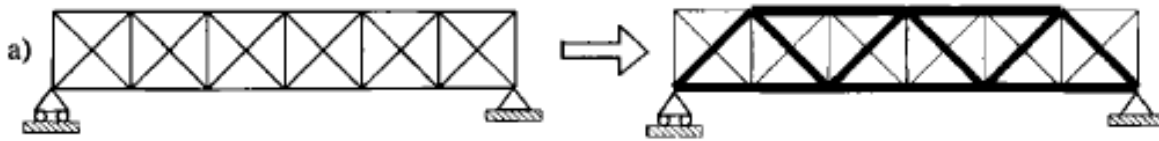


Figure 4 Size/Scantling Optimization of a Truss Structure (*Bendsoe & Sigmund, 2003*)

As stated by (Rigo, A module-oriented tool for optimum design of stiffened structures - Part I, 2001), the main design variables of size (scantling) optimization are:

- Plate thickness
- Longitudinal members – stiffeners, crossbars, longitudinals, girders, etc.:
 - Web height and thickness
 - Flange width
 - Spacing between two longitudinal members
- Transverse members – frames, transverse stiffeners:
 - Web height and thickness
 - Flange width
 - Spacing between two transverse members

In his paper, (Rigo, A module-oriented tool for optimum design of stiffened structures - Part I, 2001) develops a software, LBR-5, and its main purpose is scantling optimization of marine structures. His focus is on the “Module-Oriented Optimization” concept, mentioning that a multi-purpose optimization model, compatible with multiple codes and regulations must contain many analysis methods for strength assessment that can be easily manipulated by users. This means that the user can modify the constraints and add limitations suitable to each specific structure in the analysis process.

In this thesis, the same type of optimization technique has been approached, with a limit of design variable, being used as the main design variable the plate thickness. For this type of structural optimization, the shipyard must confirm the existence of machines and methods able to process the plates with the specific thickness defined in the optimization process.

In the paper, A Practical Method for Ship Structural Optimization (Yu, Jin, Lin, & Ji, 2010) size (scantling) optimization is named “*Property Optimization*” and described as the method whose objective is to find the structure with the minimum weight and the requirements of

strength in the whole lifecycle of the ship. (Yu, Jin, Lin, & Ji, 2010) mention that the main failure modes of a ship structure are yield, buckling and fatigue. In this thesis, the focus will be on yield strength as the main limitation of the optimization process.

In the Paper of (Yu, Jin, Lin, & Ji, 2010), a procedure for the size optimization is considered and has been adapted respectively for the use in this thesis. The solving strategy is based on the iterative process. The steps are:

1) Create the panel model as well as the FEM model with the minimum thickness. The minimum thickness is the one that satisfies the corrosion requirements in the whole lifecycle. Then apply all loads to the model for each load conditions. Calculate the current structure weight w_0 .

2) Call the solver; calculate the stress for all load conditions. For each load condition, find the stress for each node of all panels according to the corresponding stress in the FEM model. Calculate the yield criteria with considering the safety factor for the type of vessel examined and reset thickness p_i in accordance with defined yield criterion (see section 2.7.2, Eq. 14 and Eq. 15).

3) check if the yielding criterion holds. Compare stress results and weight, between initial value, before thickness reset, w_0 and, w_1 after the first iteration. If criterion 3) holds, execute 4), otherwise, execute 2).

4) Call the solver, calculate the stress for all load conditions. Then calculate the Material Utilization Coefficient

$$\mu_i = \max\left(\frac{\sigma_{i,k,s}}{\sigma_i}\right) \quad (1 \leq i \leq n_e, 1 \leq k \leq n_l, 1 \leq s \leq S_i) \quad (5)$$

where $\sigma_{i,k,s}$ is the s^{th} stress components of i^{th} element in k^{th} load condition, n_e is the number of elements, n_l is the number of load conditions, S_i is the count of valid stress components for the i^{th} element. Here, stress components include equivalent stress, $\mu_i > 1$ means the stress of the i^{th} element greater than allowable stress. So μ_i is made the foundation of yield strength.

5) If $\mu_i \leq 1$ ($1 \leq i \leq n_e$), which means all the elements meet the yield strength requirements, execute 7), otherwise, execute 6).

6) Find all elements $E = \{e_1, e_2, \dots, e_{N_j}\}$ within each panel P_j , where N_j is the elements number within P_j panel. Modify the thickness of elements in E with equation

$$t_{nsj} = \begin{cases} t_{Bmin} & t_j \leq t_{Bmin} \\ \max(t_j * \mu_{max}, t_{Bmin}) & k > 1, \text{ or } k \leq 1 \text{ and } t_j > t_{Bmin} \end{cases} \quad (6)$$

where t_{Bmin} is the thickness according to yield strength, t_j is the thickness of P_j before modification, t_{nsj} is the one after the optimization loop; μ_{max} is the maximum MUC of elements in E ,

$$\mu_{max} = \max(\mu_l) \quad (1 \leq l \leq N_j) \quad (7)$$

7) Size (scantling) optimization complete, the current thickness of each panels is the one that meets the yield strength requirements.

2.3.3. Material Optimization (Change of material grade)

Material optimization represents the method that allows the designer, or constructor (shipyard), to change the material grade, e.g. from low tensile steel to a mild or high tensile steel, depending on the ship's operation purpose and availability of optimizing the structural strength.

Material optimization is a more practical method, where the experience of the workers in a shipyard is needed as changing the type of material for panels that exceed the imposed constraints is difficult and special attention towards welding techniques is compulsory.

Another criterion for material optimization consists of the availability for the thickness of the plate. Higher-strength steel has different thickness range, as specified in section 2.7.1, therefore as mentioned, special welding techniques may be needed, increasing the production costs by more expensive labour.

2.4. The Objective of the Optimization Process

The objective of the optimization is giving better construction and operation costs while keeping an optimum structural strength. (Rigo & Rizzuto, 2003) divides optimization into two main categories:

- Basic design: where the designer can optimize the scantlings. Can be used to find out the minimal scantling for a novel ship for which the shipyard does not have previous information.

- Production design where optimization is used for the three main methods discussed at the beginning of this chapter: scantling, shape and topology optimization

In shipbuilding, it is considered that the most suitable objective function is the weight of the structure. Minimizing weight is of particular importance in deadweight carriers, in ships required to have limited draft, and in fast fine lines ships, such as passenger vessels (Rigo & Rizzuto, 2003). By considering the lowest weight solution might also represent higher production and acquisition costs, putting a spotlight on the importance of considering, along with to weight as the objective function, also the overall cost of construction of a vessel. This factor is of more importance in the present case, where cruise vessels are overly complex structures and the acquisition and labour costs are a major part of the final value.

Generally, the objective function becomes lower as the variables become larger in this optimization model, while the constraint, the yield strength, will not be satisfied until the variables are large enough.

2.5. Constraints

Rigo defines constraints as being “linear or non-linear functions, either explicit or implicit of the design variables. They are analytical *translations* of the limitations that the user wants to impose on the design variables themselves or to parameters like displacement, stress, ultimate strength, etc; the parameters being functions of design variables.” (Rigo, 2001). Rigo next classifies the constraints into three main categories:

- *Technological constraints*
- *Geometrical constraints*
- *Structural constraints*

2.5.1. Technological Constraints

Named also side constraints, they provide the upper and lower bounds of the design variables. For example, if the optimization technique used is scantling optimization, and the main design variable is the thickness of the plates, a specific range has to be mentioned. One limitation can be the manufacturing possibilities for the material used, like mentioned in section ***Linear Elastic Material Condition***, steel grade A has a lower bound of 4mm, providing a large range of opportunities for processing this type of material. These facts are validated by Rigo (Rigo, 2001), where he defined a design variable with values within $X_{i\ min} = 4mm \leq X_i \leq X_{i\ max} = 40mm$, with:

$X_{i\ min}$ – a thickness limit due to corrosion, etc.

$X_{i\ max}$ – a technological limit of manufacturing or assembly.

2.5.2. Geometrical Constraints

This type of constraints imposes relationships between design variables to guarantee a functional, feasible, reliable structure. They are based on “good practice” rules to avoid local strength failures (web or flange buckling, stiffener tripping) or to guarantee welding quality and easy access to the welds. For example, welding a plate of 30mm thickness with one of 5mm is not recommended (Rigo, 2001). Thus, a good example is to keep a limit between X_1 and X_2 design variables of $0.5 \leq X_2/X_1 \leq 2$.

A geometrical constraint can also be considered as space available on a ship. For example, if the optimization technique considered is shape optimization, as in the paper *An Approach to Optimization in Ship Structural Design Using Finite Element and Optimization Techniques*, by (Lindemann & Kaeding, 2010), their approach of optimizing the structure is by deleting sets of design variables, giving a new shape to the geometry of the structure.

In this project, the geometry of the structure is considered as a fixed constraint, therefore no changes are allowed, besides the modification of the technological design variables with consideration to structural responses.

2.5.3. Structural Constraints

Structural constraints represent the limit states to avoid yielding, buckling, etc. and to limit deflection, stress, etc. These constraints are based on solid-mechanics phenomena, modelled with rational equations based on physics, solid mechanics, strength, and stability, that differ from empirical and parametric formulations. These rational constraints are defined to limit:

- Deflection levels in the structure at different points
- Stress levels in an element (σ_x, σ_y and $\sigma_c = \sigma_{von\ Mises}$)
- Safety level related to buckling, ultimate resistance, tripping, etc. The latter ones are not considered in the present paper, the main aim is to achieve values for the yield utilisation, having considered a safety factor for the structural analysis, explained in section 2.7.2 and defined in the description of the main model, section 3.3.
- *Deflection levels at different points*

The structural constraints can be divided into local and global constraints, both being dependent on the type of loads and boundary conditions applied to the structure. Rigo mentions that local deflections must be kept at reasonable levels for the overall structure to have the proper strength and rigidity. In this thesis, the main constraints are considered at a local level, where the optimization method is implemented, and further the results are interpreted with respect to full structure.

➤ *Stress levels in an element*

Rigo (Rigo & Rizzuto, 2003) explains that to assess the equivalent von Mises stress values in elements of a panel, a superposition of stresses is needed. In a plate, each response induces longitudinal stresses, transverse stresses and shear stresses and they can be calculated individually for each response. Though this is the traditional approach considered by classification societies, and in a direct analysis like finite element analysis the separation of the responses is not possible. If they are to be calculated separately, a cumulative process has to be done for all the longitudinal, transverse and shear stresses. Still, an uncoupled procedure is convenient but does not reflect the reality and all the stresses, primary, secondary, and tertiary are superposed for the yield assessment. They are all combined in the end through a criterion, the von Mises criteria, which is usually considered in ship structures. The von Mises criteria is later explained in section 2.7.2.

The structural response of a hull can be divided into three components: primary, secondary and tertiary. The first represents the response of the hull as the ship bends as a beam under the longitudinal distribution of load. Secondary stresses relate to the global bending of stiffened panels (for a single hull ship) or the behaviour of double bottom, double sides, etc. Tertiary responses describe the out-of-plane deflection and associated stress of an individual unstiffened plate panel included between two longitudinals and two transverse web frames. Their boundaries are formed by bulkheads, web frames, stiffened panels, secondary web frames (Rigo & Rizzuto, 2003).

Primary and secondary response induce in-plane membrane stresses, nearly uniformly distributed through the plate thickness. Tertiary stresses, which result from the bending of the plate member itself vary through the thickness but may contain a membrane component if the out-of-plane deflections are large compared to the plate thickness.

Rigo & Rizzuto mention that all the methods of calculation of primary, secondary, and tertiary stress assume linear elastic behaviour of the structural material, therefore the stress

concentrations computed for the same member may be superimposed to obtain maximum value for the combined stress. In performing and interpreting such a linear superposition, several considerations affecting the accuracy and significance of the resulting stress values must be examined.

Firstly, the primary loading can be achieved by using a theory that considers a simplified concept of the hydrodynamics of ships and wave motions and the primary bending stress can be simply computed by using beam theory, giving a reasonable estimate of the mean stress in deck or bottom, neglecting localized effects such as shear lag and stress concentration.

Secondly, the three stress components may not occur at the same time as the ship moves through waves. The maximum bending moment amidships, which results in the maximum primary stress, does not necessarily occur in phase with the maximum local pressure on a midship panel of bottom structure (secondary stress) or panel of plating (tertiary stress) (Rigo & Rizzuto, 2003).

Third, the maximum values of primary, secondary, and tertiary stress are not necessarily in the same direction or even in the same part of the structure. The primary stress σ_1 will act in the longitudinal direction. The stress values will be nearly equal in the plating and the stiffeners, and approximately constant over the length of a midship panel. There exists a small transverse component in the plating, due to the Poisson coefficient.

The secondary stresses σ_2 , respective the response of the stiffened panels, which vary along the length of the panel, are usually subdivided into two parts in the case of single-hull structure. The first part, σ_2 , is associated with bending of a panel of structure bounded by transverse bulkheads and either the side shell or the longitudinal bulkheads. The second part, σ_2^* , is the stress resulting from the bending of the smaller panel of plating plus longitudinal stiffeners that is bounded by the deep web frames. The first of the secondary stresses, σ_2 , as a result of the proportions of the panels of the structure, is usually larger in the transverse than in the longitudinal direction. On the contrary, the second component is predominantly longitudinal and, in the end, the tertiary stress σ_3 happens in the plate where biaxial stresses occur. In the case of longitudinal stiffeners, the maximum panel tertiary stresses will act in the transverse direction (normal to the framing system) at the mid-length of a long side (Rigo & Rizzuto, 2003).

From this previous explanation, can be understood that the point with the highest level of stress in the structure is not immediately spotted but can be found by considering the combined stress

effects at different locations and times. As mentioned, this superposition of all the stresses is assessed directly using the Finite Element Method (FEM), where the equivalent von Mises stress is stored after the strength analysis.

2.6. Design Variables

In achieving the structural optimization necessary to reduce the weight and costs of manufacturing the ship, one or more objective functions have to be defined, and they are functions of the design variables. Also, the results upon the optimization process must follow a designated condition. In the *property optimization* technique, (Yu, Jin, Lin, & Ji, 2010), mention that the problem of optimization comes down to redistribute the thickness of the plates to make the structure weight minimize on the condition of yield strength under all load condition and this fact is backed by (Rigo & Rizzuto, 2003) statement in Chapter 18, mentioning that a ship structural design is assessed based on the acceptable stress levels compared to the yield or the ultimate strength of the material. The condition needs to be respected to check the adequacy or inadequacy of the structural member after the optimization process.

These criteria are imposed for the prevention of yielding (in hull girder, frames, longitudinals, etc.), plate and stiffened plate buckling, plate and stiffened plate ultimate strength, the ultimate strength of hull girder, fatigue, and many other types of failure particular to the type of vessel and operational scope (Rigo & Rizzuto, 2003).

In this paper, the only criteria followed is the yield strength of the material and it is described in detail in section 2.7.2.

In this thesis, as well as in the paper of (Yu, Jin, Lin, & Ji, 2010), the objective function is the reduction of the structural weight, followed proportionally by the reduction in material and manufacturing cost. The design variable considered is the plate thickness of each panel examined in the analysis with the main major constraint the yield strength of the material. Therefore, the optimization model is as follows (Yu, Jin, Lin, & Ji, 2010):

$$\begin{cases} \min & \sum_1^n weight(p_i) \\ \text{s.t.} & t_i \geq \min [yield(p_i)] \quad (1 \leq i \leq n) \end{cases} \quad (8)$$

where n is the number of panels, $weight(p_i)$ is the weight of the i^{th} panel, and $yield(p_i)$ is the minimum thickness of the i^{th} panel according to yield stress.

2.7. Steel Properties and Behaviour

2.7.1. Linear Elastic Material Condition

Isotropic linear elastic materials are characterized by their Young's modulus and Poisson's coefficient.

In engineering, the elasticity of a material is determined by two types of parameters (Elasticity (physics), n.d.):

- The material's modulus, which measures the amount of force per unit area needed to achieve a given amount of deformation; a higher modulus typically indicates that the material is harder to deform.
- The material's *elastic limit*, the maximum stress that can arise in a material before the onset of permanent deformation.

The elastic behaviour of materials is when the material is subjected to an applied force and the body is resisting to any permanent change, regaining the initial shape and size. To assess the linear elastic behaviour of a material, calculation of primary, secondary and tertiary stresses is conducted and combined for the same structural member achieving a maximum value.

According to Paik & Kim, (Paik & Kim, 2002), the material used in stiffened panels of merchant ship structures is usually mild or high tensile steel.

The materials used for this project are steel grade A and steel grade AH36. Both materials are *Linear Elastic Materials*, meaning that they obey Hooke's law, respectively the relationship between stress and strain is linear and represented by the following equation:

$$\sigma = E \varepsilon \quad (9)$$

where E is the Young's modulus, σ stress and ε strain.

Steel grade A is the common tensile strength steel and has good toughness properties and high strength, good corrosion resistance, and good processing and welding properties. It is optimum for construction of ship hull structure (Grade A shipbuilding steel plate, n.d.).

Material 1: Properties steel grade A (DNV Grade A shipbuilding steel plate, n.d.):

- Tensile, yield strength – 235 MPa
- Minimum available thickness – 4 mm

Steel grade A36 is the high tensile steel used in marine structural engineering. The material is DNV approved and is suitable for construction of- cruise vessels, ferries, yachts, but also offshore oil drilling platforms or bulk carrier hull (DNV A36 steel plate, n.d.).

Material 2: Properties steel grade A36 (DNV A36 steel plate, n.d.):

- Tensile, yield strength – 355 MPa
- Ultimate tensile strength – 490 – 620 MPa

2.7.2. Yield Criteria

In order to control the size of the plasticity zones in way of openings in highly stressed areas, local models with fine mesh need to be evaluated. Because of the geometric irregularities and the high average stresses, the local stresses in way of openings will exceed the yield strength of the material and this may cause permanent plastic deformation (DNV-GL, 2015).

In practice, a peak stress value more than yield represents a permanent strain in the material after the load has been removed. After this point, large deformations can be observed with little or no increase in the applied load, that can lead to fracture of the material (DNV-GL, 2015). Ultimate yield strength is not a matter of discussion in this paper; therefore the focus is on yield which occurs at the point of plastic deformation, a phenomenon to be avoided for this analysis.

Yield occurs therefore when the material exceeds a reference stress value and material reaches plasticity. This stress level is termed the material yield stress. While many structural design criteria are based upon the prevention of any yield whatsoever, it should be observed that localized yield in some portions of a structure is acceptable, where in reality the distribution of stresses is done towards the adjacent panels, preventing from the yield of the area. This phenomenon can be observed later in Chapter 4, where singularities have been spotted, but they do not push the structure to fail, as the overall panel average stress is below the stated yield criteria. Yield can be considered as a serviceability limit state, where a service limit state corresponds to the situation where the structure can no longer provide the service for which it was conceived. The service limit states relate to problems of aesthetic, functional or maintenance, but will not lead to the collapse of the structure. It is further explained that yield

can be assessed using basic bending theory. The main assumptions in pure bending are (Wikipedia Foundation, 2019):

- The material is homogeneous and isotropic.
- The value of Young's Modulus of Elasticity is same in tensions and compression.
- The transverse sections which were plane before bending, remain plane after bending also.

The formula to calculate the bending stress is (Rigo & Rizzuto, 2003):

$$\sigma = \frac{M}{I}y = \frac{M}{SM} \quad (10)$$

where: M – bending moment [Nm], σ – bending stress [N/m^2], I – moment of inertia about the neutral axis [m^4], y – eccentricity, or distance from the neutral axis to the extreme member [m], and SM – section modulus [m^3], where $SM = I/y$ (Rigo & Rizzuto, 2003).

The yield strength of the material, σ_{yield} , is defined as the measured stress at which appreciable nonlinear behaviour accompanied by permanent plastic deformation of the material occurs. The stress criterion that must be used is one in which it is possible to compare the actual multi-axial stress with the material strength expressed in terms of a single value for the yield. The criterion considered the most suitable for ductile materials such as ship steel is the von Mises criterion, expressed through the following equation (Rigo & Rizzuto, 2003):

$$\sigma_e = \sqrt{(\sigma_x^2 + \sigma_y^2 - \sigma_x\sigma_y + 3\tau^2)} \quad (11)$$

where: σ_e – equivalent stress [N/m^2], $\sigma_x\sigma_y$ – x and y stress components [N/m^2], τ – shear stress [N/m^2].

Moreover, it is stated that failure through yielding only occurs if the equivalent von Mises stress, σ_e , exceeds the equivalent stress, σ_0 , corresponding to the yield of the material. Therefore, a safety factor has to be assumed in order to survive the uncertain service conditions that the ships have to withstand. The formula showing the yield criterion (von Mises equivalent stress σ_e) against the permissible/allowable stress, σ_0 , upon considering the safety margin is (Rigo & Rizzuto, 2003):

$$\sigma_e \leq \sigma_0 = s_1 \sigma_y \quad (12)$$

where: s_1 – partial safety factor defined by classification societies, which depends on the loading condition and the method of analysis and σ_y – minimum yield point of the considered

material (steel). The yield strength of a material is defined upon the tensile test of a sample. The results are next plotted on a stress-strain curve and the stress at the point where the stress-strain curve deviates from proportionality is the yield strength of the material. σ_y is defined as minimum yield point as it is difficult to define the exact point at which the material will yield since materials as steel do not display an abrupt curve, but rather a range over which the yield occurs. Therefore, the minimum point of this range is considered as a minimum yield point (Matmatch, 2020).

For the calculation of the checking criteria, the DNV-GL rules have been followed, and for the cruise vessel a partial safety factor has been selected as $\gamma_R = 1.25$, based on a personal assumption, with the guidance of actual rules specified in the rules for classification of ships(DNV-GL, 2015):

$$\frac{0.98 * R_{EH}}{\gamma_R} \geq \sigma_{VM} \quad (13)$$

Therefore, the checking criteria for steel grade A is:

$$\frac{0.98 * 235 \left[\frac{N}{mm^2} \right]}{1.25} = 184.24 \left[\frac{N}{mm^2} \right] \quad (14)$$

For the simplicity of calculation, the criteria considered for the allowable stress of steel grade A is $\sigma_0^1 = 180 \left[\frac{N}{mm^2} \right]$.

Same as for steel grade A, the von Mises criterion for the higher tensile stress is:

$$\frac{0.98 * 355 \left[\frac{N}{mm^2} \right]}{1.25} = 278.32 \left[\frac{N}{mm^2} \right] \quad (15)$$

For the simplicity of calculation, the criteria considered for the allowable stress of steel grade A36 is $\sigma_0^2 = 273 \left[\frac{N}{mm^2} \right]$.

Both criteria have been considered lower than the actual calculated number, as an extra safety margin.

2.8. Load Condition

(Paik & Kim, 2002) When a ship hull is under vertical bending, panels are predominantly subjected to longitudinal axial compression in sagging, making the lower part of the vessel to stretch, respectively creating tensile stresses in the keel region and placing the weather deck in compression (USNA) or longitudinal axial tension in hogging, while bottom panels are subjected to combined longitudinal axial compression, placing tensile stresses the decks.

Upperside shells are normally subjected to combined longitudinal axial compression/tension and longitudinal in-plane bending, while lower side shells are subjected to combined axial compression/tension, longitudinal in-plane bending and lateral pressure loads (Paik & Kim, 2002).

Rigo, in (Analysis and Design of Ship Structure), classifies loads based on time duration and these categories are: static loads, quasi-static loads, dynamic loads, high-frequency loads and other loads such as accidental or thermal loads. In this paper the case considered is dynamic loads, respectively sagging and hogging wave bending moments.

Having defined the types of loads, it is important to know the location of the force acting on the ship structure in order to be able to study the response, and these classify again into local and global loads. The global, or primary loads are the ones acting on the hull girder, giving a global response. The local loads are only applied to structural members (stiffened panels, beams, plate panels, etc.). The local loads acting on a particular member also represent a contribution to the global bending moment acting on the full structure (Rigo & Rizzuto, 2003).

In evaluation of the response of the hull girder and the structural stiffening elements upon strength analysis, the worst load situation is considered, and the members are verified if they exceed any limit state. Regardless of the loading condition, whether it is sagging or hogging, the worst condition usually occurs when the wavelength is equal or almost equal to the ship's length. The two cases are explained in the following part:

2.8.1. Sagging

If the weight amidships exceeds the buoyancy or when the wave trough amidships the ship will sag, as a beam supported at ends and loaded at mid-length. It is fairly evident, that the "sagging" longitudinal bending condition is creating significant stresses in the structure termed bending stresses. The bending direction is stretching the lower portion of the structure, hence tensile stresses are being created in the keel region. Conversely, the weather deck is being placed in compression because the bending direction is trying to shorten this part of the structure (Longitudinal Strength of Ships – Hogging and Sagging Moment, 2019).

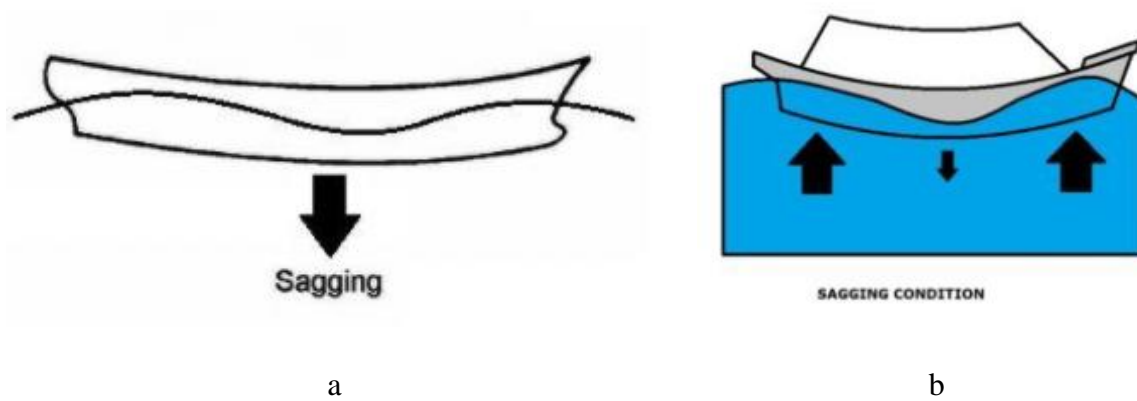


Figure 5 Sagging Bending Moment (Menon, 2020)

2.8.2. Hogging

If the buoyancy amidships exceeds the weight due to loading or when the wave crest is amidships, the ship will Hog, as a beam supported at mid-length and loaded at the end. In this condition, the overall weight is greatest near the bow and stern, with buoyancy being larger near midships. This has the effect of bending the structure in the other direction, placing the keel in compression and the deck in tension (Longitudinal Strength of Ships – Hogging and Sagging Moment, 2019).

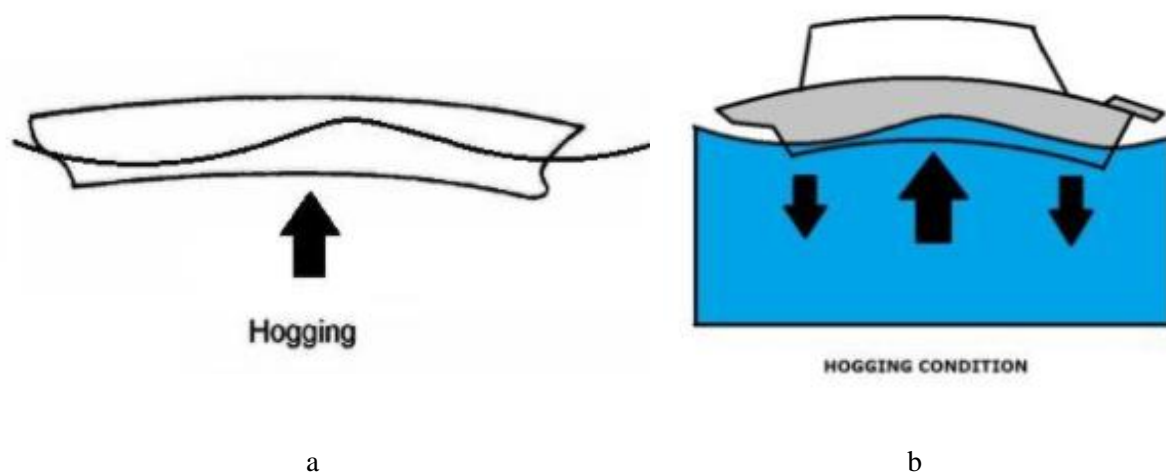


Figure 6 Hogging Bending Moment (Menon, 2020)

A ship, or a hull girder is subject to three types of loads during operation:

- Hull girder loads (global loads)
- External loads
- Internal loads (local loads)

Having these considered, and following specific rules from the Classification Society, the main strength components can be calculated, and they are (DNV-GL, 2017):

- the vertical bending moments M_{sw} and M_{wv} are positive when they induce tensile stresses in the strength deck (hogging bending moment) and negative when they induce tensile stresses in the bottom (sagging bending moment)
- the vertical shear forces Q_{sw} , Q_{wv} are positive in the case of downward resulting forces acting aft of the transverse section and upward resulting forces acting forward of the transverse section under consideration
- the horizontal bending moment M_{wh} is positive when it induces tensile stresses in the starboard side and negative when it induces tensile stresses in the port side
- the torsional moment M_{wt} is positive in the case of resulting moment acting aft of the transverse section following negative rotation around the X-axis, and of resulting moment acting forward of the transverse section following positive rotation around the X-axis

These sign conventions for these forces and moments are shown below, in Figure 7 :

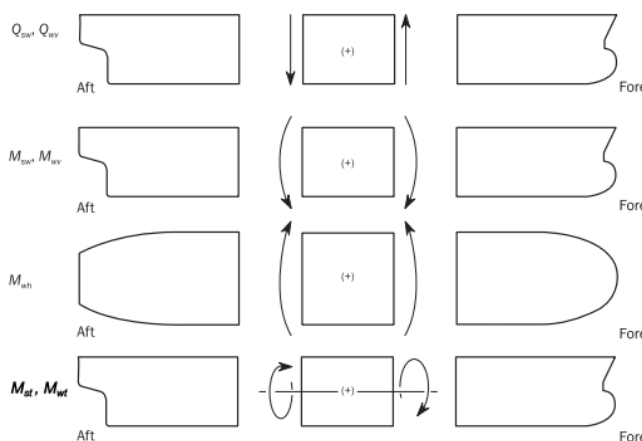


Figure 7 Sign Convention for Shear Forces and Bending Moments (DNV-GL, 2017)

3. NUMERICAL MODEL

Cruise vessels are structures with the scope of tourism, where passengers spend time, live, and have part of entertainment while the crew has to make sure their services are the best, assuring passenger's return for another lifetime experience. An important aspect when talking about cruising is the safety on board where the designers and people behind the construction of these giant structures have to make sure the vessel complies with all the structural rules. Moreover, good structural design means an optimized structure that can withstand the loads it has been designed for, by managing to reduce structural weight to reduce operational and production costs. As Yu et. al. (2010) mention in their paper, the structure model is the foundation of structure optimization based on FEM. For yield strength, the stress is calculated directly by the FEM model, so the FEM model is essential (Yu, Jin, Lin, & Ji, 2010).

For the optimization process analyzed in this project, a numerical model is needed to perform strength analysis via finite element analysis (FEM). In the first instance, a sample model has been developed in order to simplify the testing of the developed algorithm. The sample model is described further in section 3.2. Secondly, the main model is analyzed. It comprises of a mesh model of the cruise vessel subjected to numerical optimization analysis. For this part, a smaller section has been selected for the implementation of the algorithm and more details are revealed in section 3.3, where the main model is described.

The objective of the numerical model is as mentioned to simplify the implementation of the optimization algorithm and to ease the tracking of the limitations imposed to the structure, such as stress limitations (structural constraints), geometrical constraints and technological constraints. The smaller model used helps identify the change in thickness for the optimization process and this is possible by plotting the different thicknesses in different colour codes, each representing one individual value. In the end, the results of the objective functions mentioned in section 2.4 will be analysed and in the next chapter, a thorough investigation of the results is detailed.

In order to assess all these, as specified in the previous paragraphs, an optimization algorithm has been developed and in this chapter, the process is explained thoroughly in section 3.4.

In this thesis, all the numerical simulations have been performed with ANSYS APDL (Ansys®), as mentioned in the introduction. The procedures followed are explained in the

following sub-chapters, starting with the general layout of ANSYS Mechanical APDL (Ansys®) version 18.2, Research version, that has been used to fulfil this project.

The present chapter provides:

1. Short description of the necessity of numerical analysis for the optimization process and the procedure followed.
2. ANSYS Parametric Design Language – the general layout of the ANSYS Mechanical APDL is presented, explaining the characteristics of interest that have led to the fulfilment of this project.
3. Sample Model Description - An initial model generated to facilitate the macro development.

Main Model Description – The description of the main model subjected to structural optimization in this thesis.

3.1. ANSYS Parametric Design Language (APDL)

ANSYS Parametric Design Language or short APDL is a powerful scripting language that allows the user to parametrize the model and automate common tasks. The main capabilities of APDL are (UNICAMP):

- Input model dimensions, material properties, etc. in terms of *parameters* rather than numbers
- Retrieve information from the ANSYS database, such as a node location or maximum stress.
- Perform mathematical calculations among parameters, including vector and matrix operations.
- Define *abbreviations* for frequently used commands or macros.
- Create a *macro* to execute a sequence of tasks, with if-then-else branching, do-loops, and user prompts.

The most used characteristics of APDL for this project were retrieving of information from ANSYS database and creation of macros that can automate common processes useful in the optimization process, such as retrieving of stress and displacement values, as well as section IDs of the plate thickness and the material IDs existing in the model.

ANSYS Mechanical APDL supports definition of scalar parameters and arrays and the latter are defined in the project and used in retrieving the necessary parameters needed for the FE Analysis of the structure.

3.2 Sample Model Description

A sample structure has been developed in ANSYS Mechanical, using the APDL scripting, to help establish the optimization algorithm. The purpose of this sample model was to provide the developer with a smaller structure, with the necessary structural elements to test and implement the optimization technique. It comprises of 261 stiffened panels, that present a discretization of 600x600mm mesh elements. The material used is steel with an elasticity modulus $E=2.06 \cdot 10^5$ MPa, Poisson ratio $\nu = 0.3$ and material density $\rho = 7.85 \cdot 10^{-9}$ kg/mm³.

The implementation of this model was necessary to ease the testing of the algorithm. In order to check if the optimization method is correct, a trial and error approach has been conducted. For this, many simulations have occurred, and the process required a large amount of time to run an optimization iteration, verify if the results comply with the imposed constraints, and if required, a modification would be appointed. Therefore, loading the main model from the beginning would have been a time-consuming process, resulting in the algorithm to be costly from the computational point of view.

As explained in the previous paragraph, the structure consists of well-bounded stiffened panels, which makes it a quite stiff structure to optimize. Hence, the dimension made it easier to check in detail the progress of the code development. The model and a part of the stiffened panels can be observed in Figure 8.

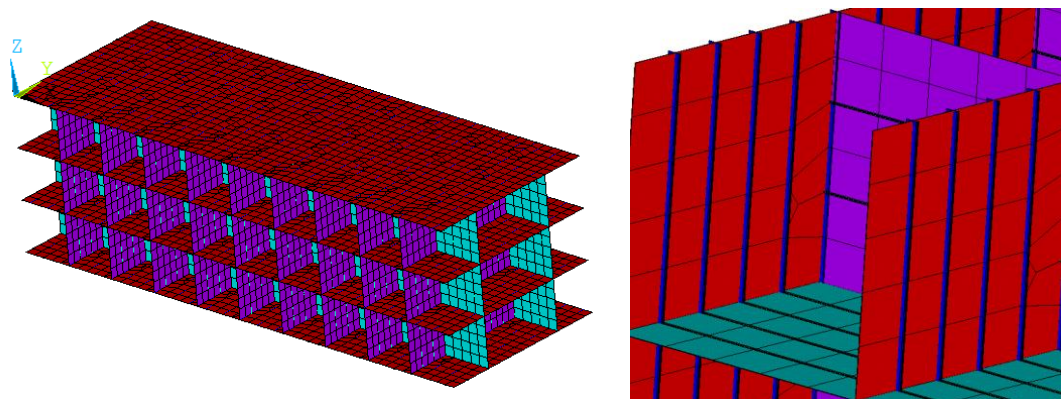


Figure 8 Sample model structure and stiffened panels in the structure

3.2.1 Boundary Conditions and loads

In the sample structure, the material is linear elastic, and the panels are simply supported. This results in fixed translations and rotations at the edges of the panels. In the left part of *Figure 9* there are the boundary conditions, where the yellow and blue ones are the essential boundary conditions, respectively fixed rotations (yellow) and fixed translations (blue). The red arrows represent the natural boundary conditions comprised of forces and accelerations. In the right figure, the arrows represent the loads, respectively the forces and reactions. Here the green arrows represent the moments with their reactions in dark purple and the pink arrows represent forces and respective reactions.

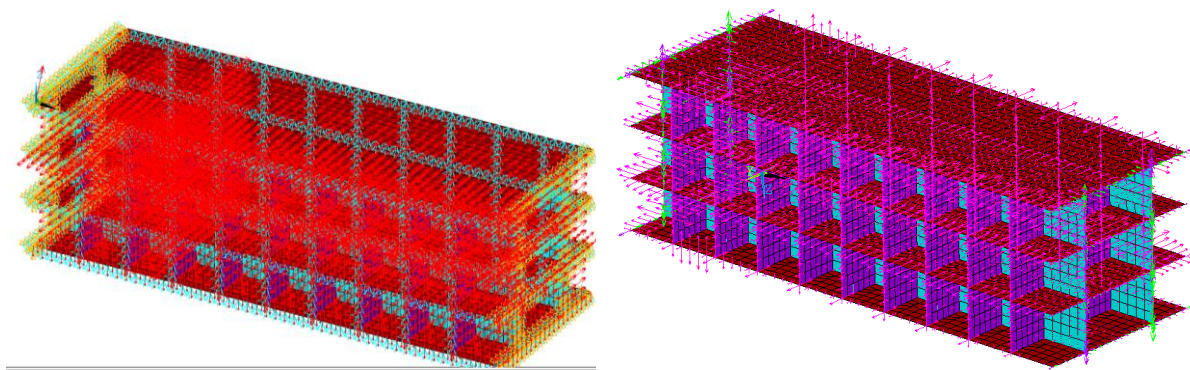


Figure 9 Boundary conditions and reactions on the sample model

3.3 Main Model Description

The structure set for analysis is a cruise vessel of an approximate length of 340 m, that can accommodate a maximum of 9500 passengers on board, with an average of 5000 when the maximum load-carrying capacity is not required (off holiday season) (MV WERFTEN Wismar, n.d.). In Figure 10 the finite element model of the vessel is visible, along with the coordinate system.

Similarly to the sample model, for the implementation of the optimization algorithm which has been developed with the use of the sample structure, from the main model has been selected an area of 440 panels, shown in Figure 10 by the yellow rectangle bounding the area. The selected part is on the full width of the vessel, selected from the double bottom, to avoid the curved panels in the bilge area up to the sixth deck.

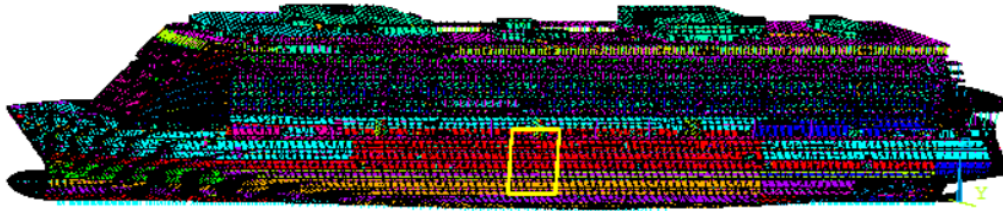


Figure 10 FEM Model of Main Structure – Cruise Vessel (MV WERFTEN Wismar, n.d.)

The model provided gives information only related to the types of elements defined, SHELL 181, BEAM 188, LINK 14, COMBIN; element mesh (discretization), section ID (thickness sections) and material properties, such as Young's modulus, Poisson's ratio and density of the material. The model has a total of approx. 248800 elements, divided into the 4 types mentioned beforehand.

The SHELL 181 element is suitable for analysing thin to moderate thick shell structures. It is a four-node element with six degrees of freedom at each node: translations in the x, y and z directions and rotations about the x, y, and z axes. It is well-suited for linear applications and change in thickness is possible (SHELL 181, n.d.). BEAM 188 is suitable for analysing slender to moderately stubby/thick beam structures. The element is based on the Timoshenko beam theory which includes shear-deformation effects. It is a linear, quadratic, or cubic two-node beam element in 3D. This type of element has six degrees of freedom (DOFs), same as the SHELL 181 element (BEAM 188, n.d.).

In DNV-GL rules (DNV-GL, 2015), it is stated that in order to determine the normal and shear stress responses of the hull girder, direct strength calculations using FEM (finite element method) is required, as there are multiple decks and openings in a cruise vessel.

Another reason for selecting one specific region of the ship is that the structural analysis to be performed for the entire vessel in one computation is highly expensive, requiring many resources and a high amount of time. Therefore, a section in the midship area has been selected (see Figure 11) to better emphasize the behaviour of the ship on the two loading conditions (extreme cases sagging and hogging) and facilitate the outcome and interpretation of the results for the structural optimization process.

The structure examined for the optimization is shown below in Figure 11. The palette of colours present on the panels of the section are the different thickness values considered in the initial case of the structure. Each colour represents one section ID defined in the ANSYS database of

the model. The model is composed of 6 (six) decks, 2 (two) transversal bulkheads and 2 (two) longitudinal bulkheads, comprised in a total of 440 panels.

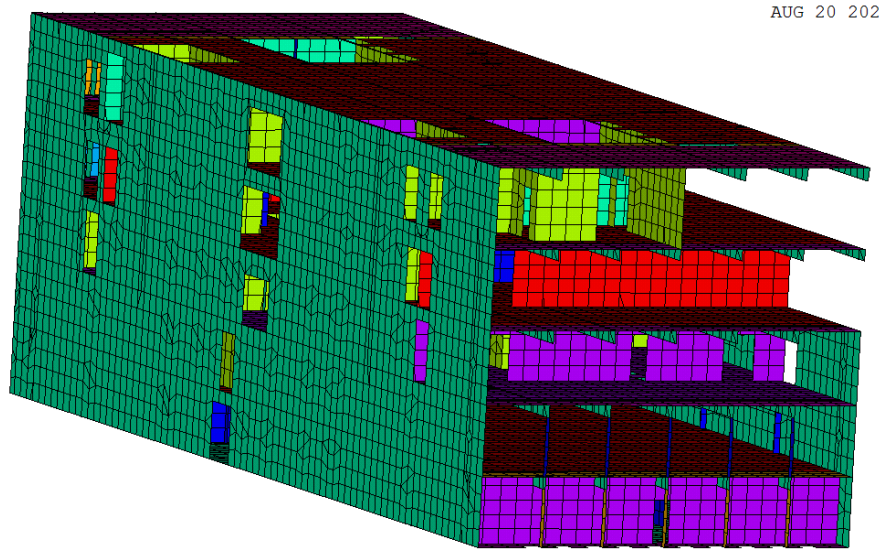


Figure 11 Section of the vessel considered for structural optimization

In Analysis and Design of Ship Structure (Rigo & Rizzuto, 2003) the ship structure is referred to as a box girder, a hull girder. To model the hull girder, structural main components are needed, and these are stiffened panels. The stiffened panels usually consist of a plate with stiffeners, transverse frames or girders attached to it with the purpose of strengthening. These are defined after the main dimensions of a ship are set, and the scantling process can be initiated, as the panels are strengthened by longitudinal or transversal stiffening members.

The stiffened panels are comprised of longitudinal and transversal stiffening and explained below (Rigo & Rizzuto, 2003):

- Longitudinal Stiffening – includes:
 - longitudinals – equally distributed – used for the design of longitudinally stiffened panels
 - girders – not equally distributed
- Transverse Stiffening – includes:
 - Transverse bulkheads
 - The main transverse framing – equally distributed with large spacing – used for both longitudinally and transversally stiffened panels.

An example of a stiffened panel can be observed in Figure 12.

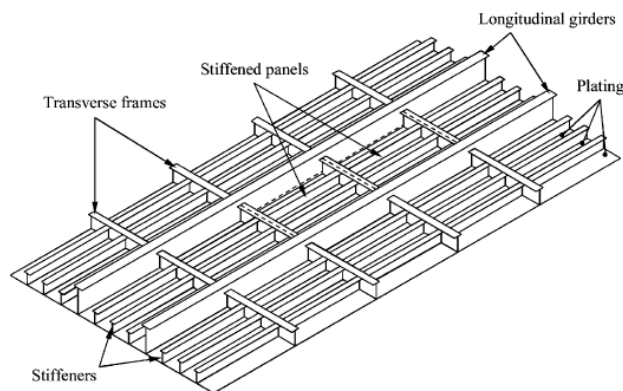


Figure 12 Stiffened plate structure (*Paik & Kim, 2002*)

3.3.1 *Boundary Conditions and Loads*

There are two types of boundary conditions to be considered, the first is the essential boundary conditions, which impose specific values to the variables at the boundary. They are imposed explicitly for the solving of the model and are related to the degrees of freedom (DOFs), respectively translational and rotational constraints. In this case, the panels in the structure are simply supported, imposing restrictions of displacement and rotation. The second type is natural boundary conditions they are related to the bending moments and shear forces in the stress analysis. For this model, this would be the two main loading cases considered, sagging and hogging bending moments (Caendkoelsch, 2018).

The loading condition considered are sagging and hogging bending moments and due to these extreme situations, the area selected for the analysis is the midship section of the vessel, where realistic values can be expected, in comparison to the extremities of the ship. The boundary condition and loading distribution are shown for the global model in Figure 13 and the local model, in Figure 14. The green arrows represent the moments, whereas the red ones represent the forces acting on the vessel. There are also visible the imposed constraints on the displacement, in light blue, and the pink arrows which represent the reactions.

U
F
NFOR
NMOM
RFOR

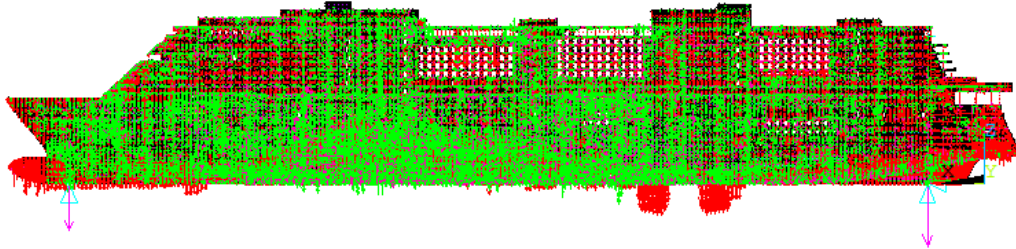


Figure 13 Coupled boundary conditions and loads acting on the ship

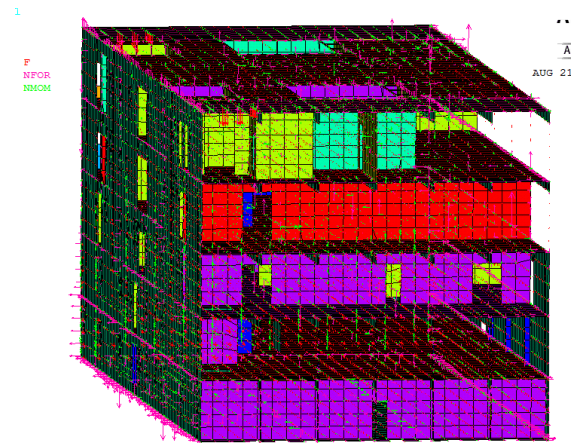


Figure 14 Boundary conditions and loads acting on the selected structure

3.4 Algorithm Development

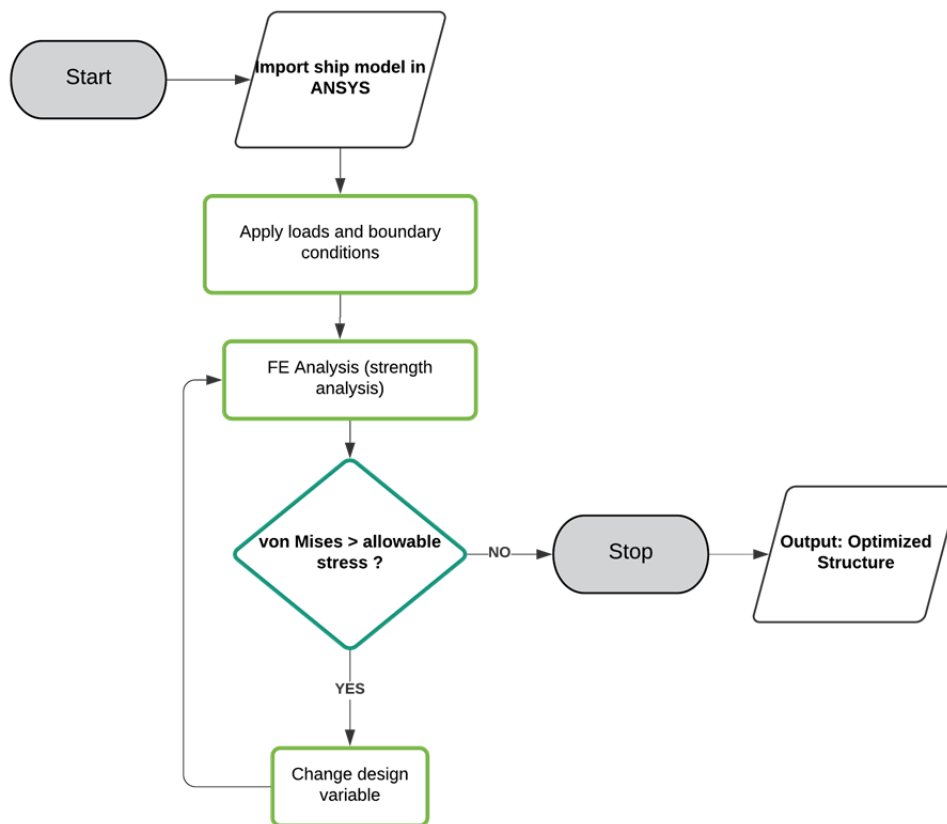


Figure 15 Optimization Algorithm

After launching ANSYS Mechanical Academic Research and CFD, version 18.2, the first step is to load the model of the cruise vessel shown previously, in Figure 10, and to uniformly decrease the thickness of the full vessel to 4mm, in order to have a more suitable structure for the optimization process, respectively, weakening the structure provides more panels that will exceed the constraints. Secondly, the loads and boundary conditions are applied to the model and the solver is called, in order to perform the strength calculation.

For the optimization process, the selected part of the vessel has been chosen to have less computational expense and the results can be processed easier than considering the full model. Therefore, after having solved the model, the panel list of the 440 panels is run as a command in ANSYS Mechanical and the coordinates of the panels are stored into an ANSYS array, which will further guide the storing of the stress values for each panel.

The next step is to read the stress values, which are stored in a result table as average equivalent von Mises stress per each panel. After this, the next crucial step in the optimization macro is to define the stress criteria upon which the panels will be optimized. This criterion, it is, as defined in section 2.7.2, $\sigma_0^1 = 180 \text{ N/mm}^2$ for steel grade A and $\sigma_0^2 = 273 \text{ N/mm}^2$ for steel grade A36.

In the development of the optimization algorithm, two methods have been implemented, one considering the change of the thickness of the panel as an optimization measure, and the second considering the change of the material grade as a more practical optimization measure for a shipyard.

For the first method, one macro (code) has been developed to read the panels that exceed the stress criteria and impose to those panels an increase in thickness by +1 mm for each iteration. Therefore, after having completed one iteration, new stress results will be stored in the results array and the optimization macro is called again, where the new stresses are compared to the criteria and if there still are panels exceeding the yield criteria, an additional 1mm will be added to the panels failing. After this step, the solver is called again, where the loads are re-distributed to give more accurate results considering the new thicknesses and the strength calculation is carried once more. This iterative process continues until the stresses are no longer exceeding the criteria imposed a priori.

In the second case, the first steps in the optimization are similar, therefore the stress values of each panel at the initial loading condition (sagging or hogging) are stored in an array, based on which, the panels with a utilisation factor higher than 1, are assigned for material change from steel grade A to steel grade A36, respectively from normal shipbuilding steel, to higher tensile steel.

4. NUMERICAL OPTIMIZATION ANALYSIS

4.1 Change in Plate Thickness

Starting from the size optimization method explained in Chapter 2, sub-sub-chapter 0, in this section the results of the analysis will be presented, showing how the geometrical, technological and structural constraints have been assumed in the structural optimization process.

Vital in the process of size (scantling) optimization, where the focus is on changing the thickness of the panels based on the yield criterion defined a priori, are the stress values, respectively the von Mises criterion. The model provided, previously shown in Chapter 3, section 3.3, has proven to be heavily stiffened and only two panels would exceed the yield criteria of the material, and not with much above the limit. For optimization purposes, the thickness of the entire vessel has been changed to 4mm, in order to give better stress values, hence a better structure to optimize. This change can be seen in Figure 16, where on the left there is the model at the initial condition, as provided from the shipyard, and on the right, there is the model with the new initial condition, which is at 4mm thickness uniformly distributed along the structure.

Below in Figure 17, there is shown that each panel has a new thickness assigned, as seen in the change in colour, but also the section ID displayed on the elements, respectively the section for the 4mm thickness.

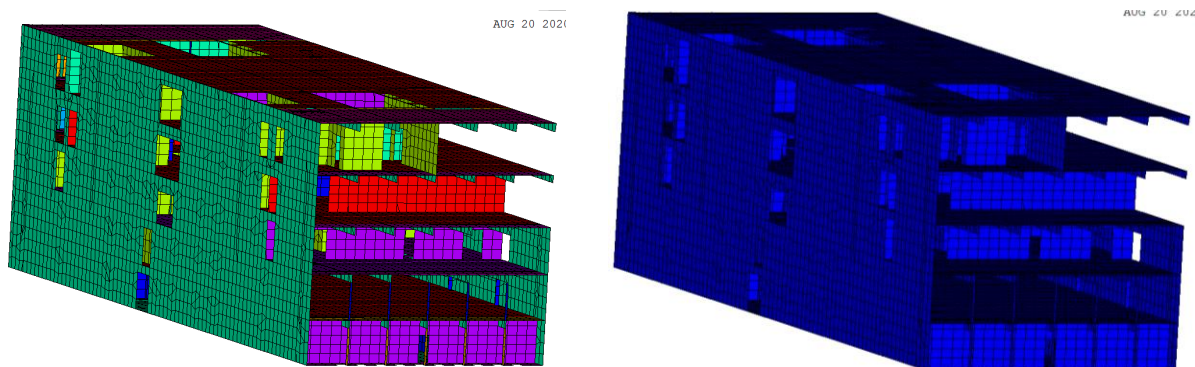


Figure 16 Comparison between structure at initial condition and section with changed thickness to 4mm

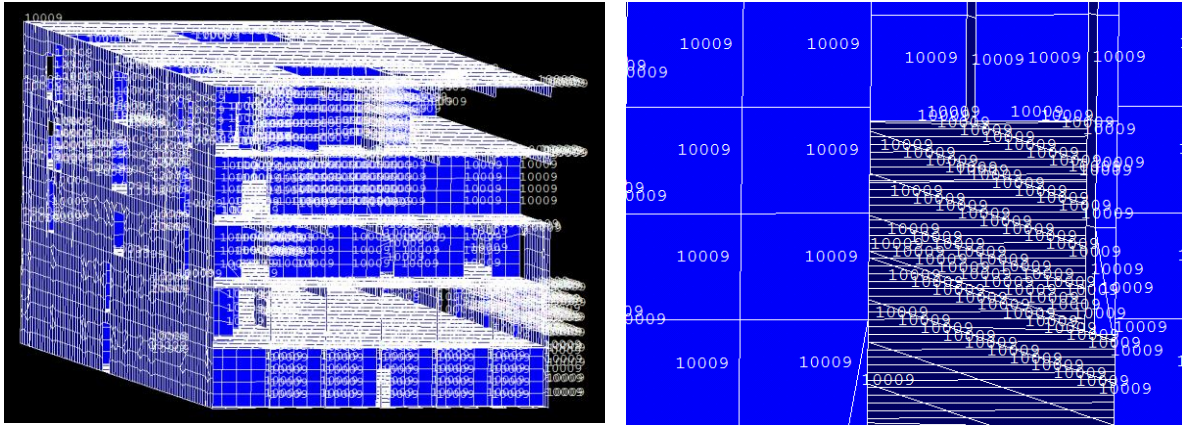


Figure 17 Section ID of thickness 4mm

From Eq. (13) it is then possible to estimate the strength criteria used for the current analysis.

Based on DNV-GL rules, as mentioned in section 2.7.2, the partial safety factor chosen is $s_1=0.784$ for the yield strength of the grade A steel, $\sigma_y = 235 \left[\frac{N}{mm^2} \right]$, resulting in an allowable stress $\sigma_0^1 = 184.24 \left[\frac{N}{mm^2} \right]$, and for steel grade A36, $\sigma_0^2 = 278.32 \left[\frac{N}{mm^2} \right]$. For the simplicity of evaluation and higher safety provided in the calculations, the final allowable stresses are $\sigma_0^1 = 180 \left[\frac{N}{mm^2} \right]$ and $\sigma_0^2 = 273 \left[\frac{N}{mm^2} \right]$.

Up to this point, the details provided are commonly followed for both loading cases, sagging and hogging. Next, the optimization considering the sagging loading case is detailed and in the hogging condition, the results are shown in the form of graphs only. The detailing of hogging case is longer, and since the approach is the same, for this loading condition there will be provided only the results in section 4.3.2 with explanatory graphs.

4.1.1 Sagging

The structure provided by the company is well defined, therefore the loading condition does not influence the structural members to yield. Therefore, as explained previously, the thickness has been changed uniformly to 4mm, to have a better-defined model on which to implement the optimization algorithm. Therefore, in the left part of *Table 1*, the values depict the largest stress values in the local structure before the thickness change to 4mm, and in the right, the stress values are resulting from uniformly changing the thickness of the model to 4mm. This means an increase of stresses of up to two times larger than the initial case. The new structure depicts now values of equivalent stress large enough to understand that yield occurs in some of the panels.

Table 1 Weakening of the structure - Uniform thickness of 4mm

Initial Case				Structure at 4mm			
Panel No.	von Mises [N/mm ²]	Initial section ID	Thickness [mm]	Panel No.	von Mises [N/mm ²]	New section ID	Thickness [mm]
140	146.8575	759	8	140	305.5719	10009	4
150	134.7996	761	6	150	263.4566	10009	4
166	120.3295	759	8	166	247.5059	10009	4
136	118.9838	762	7	136	245.3402	10009	4
218	107.6282	768	5	218	166.8083	10009	4
151	104.5388	761	6	151	203.3767	10009	4
135	104.1313	762	7	135	221.4129	10009	4
160	101.378	761	6	160	185.8419	10009	4
217	99.72547	768	5	217	155.8054	10009	4
141	95.28325	759	8	141	211.3334	10009	4

Table 2 Difference in [%] of stresses between initial case and structure at 4mm

Panel No.	Difference [%] of σ_{VM}
140	108.1%
150	95.4%
166	105.7%
136	106.2%
218	55.0%
151	94.5%
135	112.6%
160	83.3%
217	56.2%
141	121.8%

The changes that occurred before the optimization algorithm are visible in Figure 16.

First Iteration

In the first iteration in the sagging loading condition, the panels exceeding the criteria imposed of 180 N/mm², will be subjected to thickness change and in this first scenario, the 4mm panels will be modified to a new thickness, respectively to 5 mm. The number of panels yielding, in this case, is eight. The change is visible in Figure 18 where the optimized panels are selected in the red square.

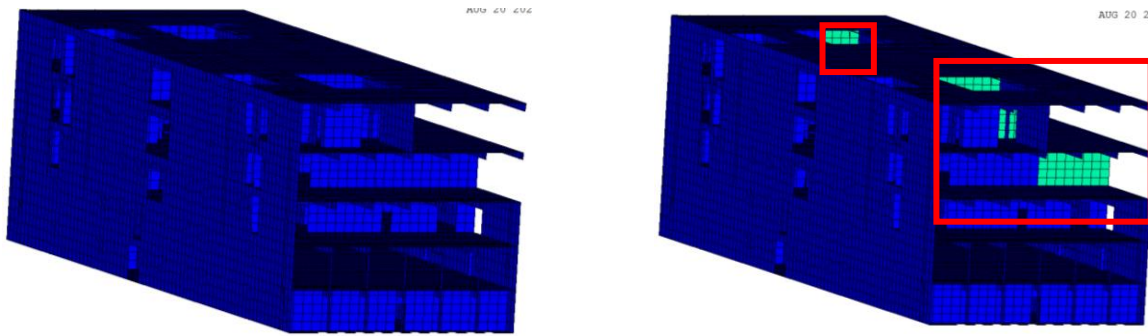


Figure 18 Comparison between initial structure and structure after the first iteration

After the first iteration, the panels displayed in green in the figure above have had their thickness updated from 4mm to 5mm. This has led to a decrease in structural stresses of maximum of 12.1 %, as explained in Table 3. Although a large change has occurred in some of the panels, there are still panels which were not yielding, even after the modification to the new structure. Despite this, panels 217 and 218 have a slow decrease in stresses, provided the positive impact of the algorithm.

Table 3 Difference in [%] of the stress values in panels

Panel No.	Difference [%] of σ_{VM}
140	-10.6%
150	-11.9%
166	-12.1%
136	-8.3%
218	-0.9%
151	-13.5%
135	-10.0%
160	-12.1%
217	-0.8%
141	-12.2%

Second Iteration

In the next stage, the iteration starts with six panels failing, which leads to understanding that after the first iteration, 2 panels have been optimized and they no longer fail by yielding. Now the panels whose stresses exceed the criteria of $\sigma_0^1 = 180 \left[\frac{N}{mm^2} \right]$ will have the thickness increased from 5mm to 6mm. The changes that occurred after the thickness change are shown in the different colours attributed to the panels analysed. In Figure 19 we can see that the majority of panels that were optimized in the first iteration, are light green (left picture) and

some of the same panels that have failed the criteria, have been optimized in the second iteration, and they can be observed as light blue colour, respectively the area bounded by the red line.

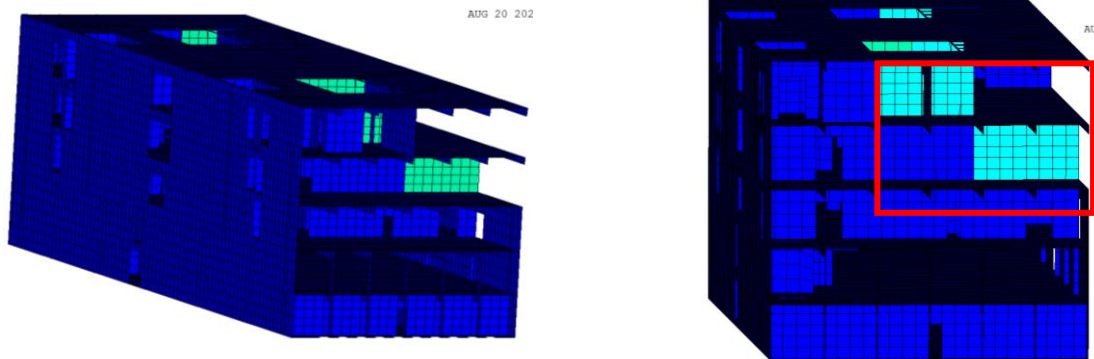


Figure 19 Comparison between first and second iteration

Again, a visible difference occurs in the stress values after the optimization method has been implemented, and this change can be assessed as before in percentage, to give a better view over the magnitude of the modifications. Hence, the majority of panels that were yielding in the model have their stresses decreased up to a maximum of nearly 11%.

Table 4 Difference in [%] of stress in panels after the second iteration

Panel No.	Difference [%] of σ_{VM}
140	-10.1%
150	-10.8%
166	-10.4%
136	-7.2%
218	-0.3%
151	-0.9%
135	-8.7%
160	-0.4%
217	-0.4%
141	-10.3%

Third Iteration

In the third iteration, starting with five panels yielding, the same optimization algorithm is implemented, by considering the material limitation of 180 N/mm^2 and by updating the thickness of the failing panels by adding 1mm thickness more, respectively to 7mm.

The five panels exceeding the limit stated above have changed thicknesses from 6mm to 7mm. The panels that were in a safe range have kept the initial values of the mentioned variables and some have slightly changed stress values, due to the behaviour of the structure subject to analysis, e.g. panel 141, where an increase of 0.2% in equivalent stress has occurred.

Nevertheless, the modifications are noticed in the images plotted from ANSYS Mechanical, and for this case the panels that have suffered modifications come in purple colour, distinguishing from the previous iteration.

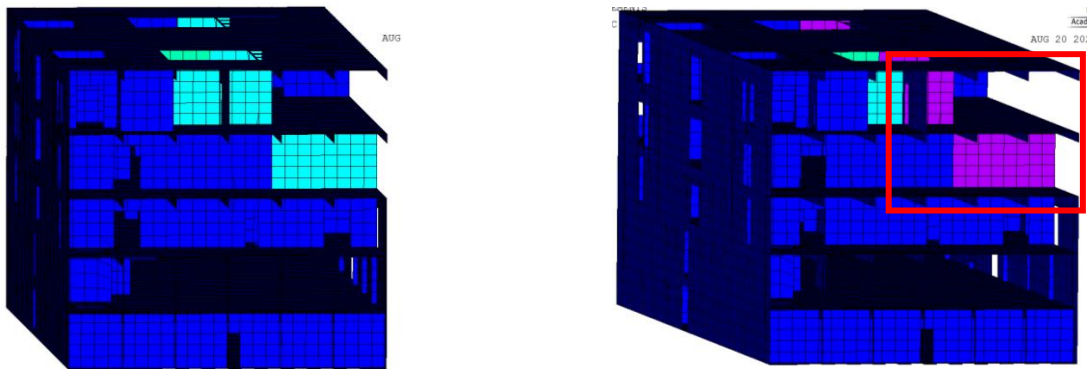


Figure 20 Comparison between second and third iteration

The difference between the stresses in the second and the third iterations are noted in percentage equivalents. As explained previously, panel 141 has its stresses increased by 0.2% due to the behaviour of the structure subjected to boundary conditions and sagging bending moment.

Table 5 Difference in [%] of stress in panels after the third iteration

Panel No.	Difference [%] of σ_{VM}
140	-9.4%
150	-9.5%
166	-9.2%
136	-6.7%
218	-0.2%
151	-0.6%
135	-7.9%
160	-0.3%
217	-0.3%
141	0.2%

Fourth Iteration

Now the optimization is down for 3 panels, and although subject to change are the panels failing the criteria, the optimization loop regards all the panels and all the changes that occur after each iteration. Therefore, this stage considers the change from 7mm to 8mm of the panels that still yield.

Here, the changes can be spotted in Figure 21, where the newly optimized panels display a red colour. At this point of optimization, a variety of new thicknesses are present in the optimized structure, as they depend on the influence of load distribution and boundary conditions.

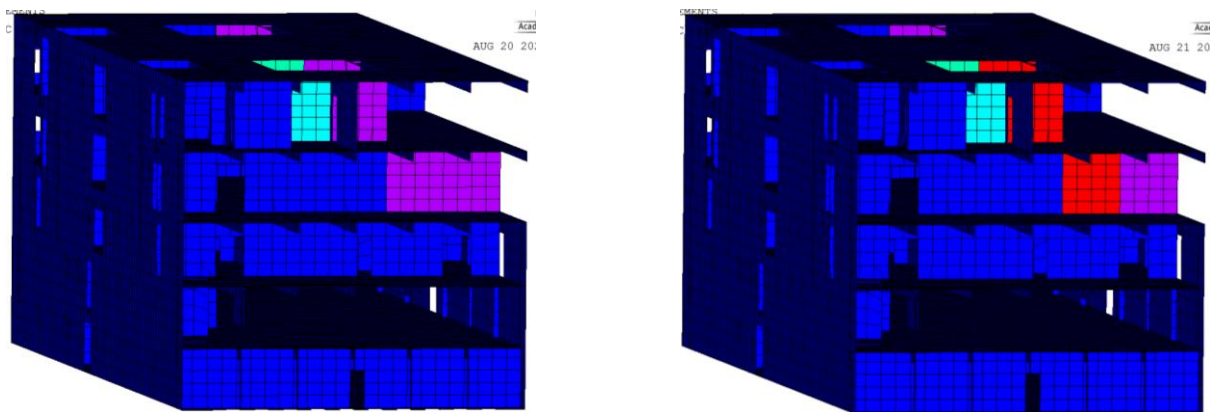


Figure 21 Comparison between third and fourth iteration

Again, the stress differences are observed in Table 6, where large decrease has occurred in panels 140, 150 and 136, a small increase is noticed in panels 135 and 141, and the rest have a small decrease. All these changes are generated by the thickness update by 1mm and the overall behaviour of the structure under boundary conditions and loads.

Table 6 Difference in [%] of stress in panels after the fourth iteration

Panel No.	Difference [%] of σ_{VM}
140	-8.70%
150	-8.51%
166	-0.06%
136	-6.93%
218	-0.10%
151	-0.51%
135	1.60%
160	-0.11%
217	-0.05%
141	0.02%

Fifth Iteration

In the fifth stage, two more panels are to be optimized, panel 140, giving the largest stress in the entire model, and panel 136, that is only exceeding the limit by 0.7%. Nevertheless, the thicknesses of these two panels are modified by adding 1mm more to the panel's thickness.

This thickness change comes shown in Figure 22, framed by the red square. By comparison with the structure at the previous iteration, all the panels that have been optimized during the process display a different colour and the diversity increased up to this point where the two panels have changed their thickness to 9mm.

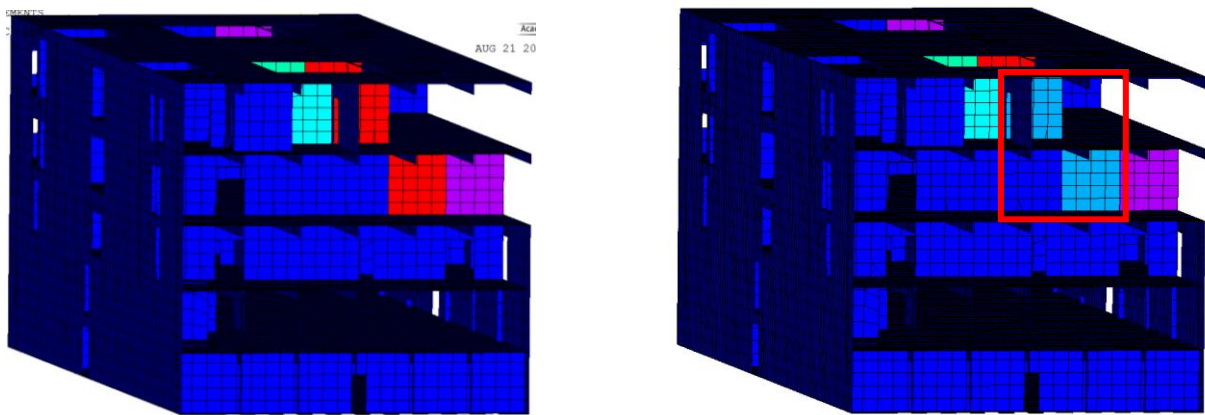


Figure 22 Comparison between fourth and fifth iteration

Panel 136 has been optimised, by reducing the stress values by 6.15% compared to the previous iteration and the panel with the largest value has been optimized by a difference in the stress of 8.1%, still exceeding now only by almost 7 N/mm², the limit criteria.

Table 7 Difference in [%] of stress in panels after the fifth iteration

Panel No.	Difference [%] of σ_{VM}
140	-8.10%
150	-0.27%
166	-0.02%
136	-6.15%
218	-0.04%
151	-0.21%
135	1.41%
160	-0.05%
217	-0.03%
141	0.19%

In practice, another iterative step might be expensive to implement, therefore, since the allowable criteria has been selected lower than the actual yield criteria including the partial safety factor, it is safe to assume that the optimization process can be stopped after 5 iterations. For accurate results in this study, the last iteration has been performed to confirm that the structure has reached an optimized level.

Sixth Iteration

The sixth iteration, which is the last in this optimization case, with the structure subjected to sagging bending moment is analysing only one panel (panel 140) whose stress value is exceeding the limit of 180 N/mm^2 . Therefore, in Table 8 panel 140 shows reduced stress on the right side of the table, by nearly 8 N/mm^2 . This result has been achieved by changing the thickness of panel 140 from 9mm to 10 mm.

Table 8 Sixth iteration - change in thickness - Sagging

Sixth Iteration							
Panel No.	von Mises [N/mm ²]	Section ID	Thickness [mm]	Panel No.	von Mises [N/mm ²]	Section ID	Thickness [mm]
140	186.6917	10014	9	140	178.664	10015	10
150	170.8647	10013	8	150	170.8606	10013	8
166	176.8681	10012	7	166	176.8679	10012	7
151	170.1166	10014	9	151	170.1171	10014	9
141	164.2313	10009	4	141	164.2303	10009	4
167	172.0224	10010	5	167	172.0231	10010	5
160	172.5315	10012	7	160	172.5314	10012	7
436	161.9142	10010	5	436	161.9088	10010	5
169	153.3732	10009	4	169	153.3616	10009	4
168	167.2796	10011	6	168	167.28	10011	6

Once again, the modification of the thickness is visible in Figure 23, where only one panel is framed in red, displaying the difference from 9mm to 10mm, respectively.

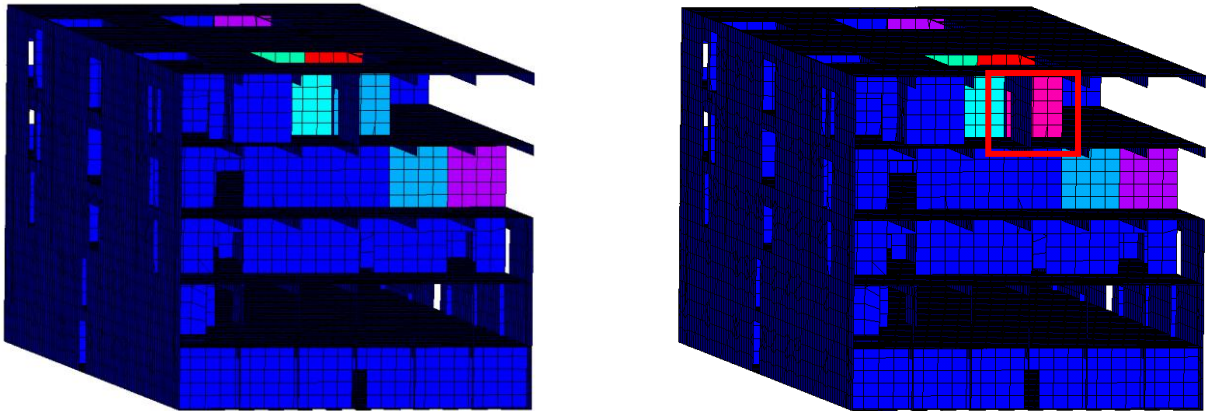


Figure 23 Comparison between fifth and sixth (last) iteration

In this last optimization step, the stress in the panels suffer changes in both positive and negative ways. For example, even if the optimization process has the meaning of reducing stresses in panels, there are few sections in which, due to influence of the behaviour of the hull girder, the stresses are increasing by very low values such as, 0.3%, 0.4% and 0.2%. These are acceptable values as the average stress value of the panel does not exceed the constraint imposed from the beginning.

Table 9 Difference in [%] of stress in panels after the sixth iteration

Panel No.	Difference [%] of σ_{VM}
140	-4.30%
150	-0.24%
166	-0.01%
136	0.03%
218	-0.06%
151	0.04%
135	-0.01%
160	-0.33%
217	-0.76%
141	0.02%

The output of this optimization loop comes with a structurally optimized model. Not only the panels no longer yield, but some of the panels can withstand more loads by maintaining a good structural integrity. The newly optimized structure will have an impact on the overall weight,

where, as explained in the theoretical chapter, by optimizing one objective function, the second might have negative outcome. This is explained further in the results section of this chapter.

4.2 Change in Material (Steel) Grade

The second optimization method considered for this project is a more practical approach used by the shipyards, where the material of the panels exceeding yielding criteria is changed to a more resistant material. In this case, the study is performed considering steel grade A as normal steel, with the yield strength $\sigma_{y1} = 235 \text{ N/mm}^2$, and steel grade A36 as high tensile steel, that can withstand stresses up to $\sigma_{y2} = 355 \text{ N/mm}^2$. For both the materials, a safety factor of 0.784 has been considered, lowering these values to $\sigma_{e1} = 180 \text{ N/mm}^2$ and $\sigma_{e2} = 273 \text{ N/mm}^2$.

Since the vessel under analysis is a cruise vessel and the main important aspect, in this case, is the structural integrity that can assure the passengers that the ship is strong enough for severe cases, the safety factor has been chosen above the stated limit of 1.2 mentioned by the classification society, as mentioned in the paragraph below, $SF = 1.25$.

In both sagging and hogging loading conditions, the panels would not fail by yielding, as shown previously in the thickness change section. For the optimization algorithm to have a testing ground, the thickness of the full vessel has been changed to 4mm uniformly. After this, strength analysis has been performed and after evaluation of the stress values in each panel, the material has been changed or kept accordingly.

Sagging

In the sagging case, as presented in the previous section of results, no panel will fail by yielding and this is visible in Figure 24 on the left, where all the panels usage is less than 1. To assess this method, a change in structure has been forced, respectively a redistribution of the thickness as such the model to have 4mm uniform thickness. After this modification, the usage factor is computed once more and the changes that occur are described by the figure on the right, where the red panels have usage factor values higher than one, resulting that these panels will yield. This fact is also depicted in the results of Table 10, where the stress values of the initial case and after changing thicknesses can be observed.

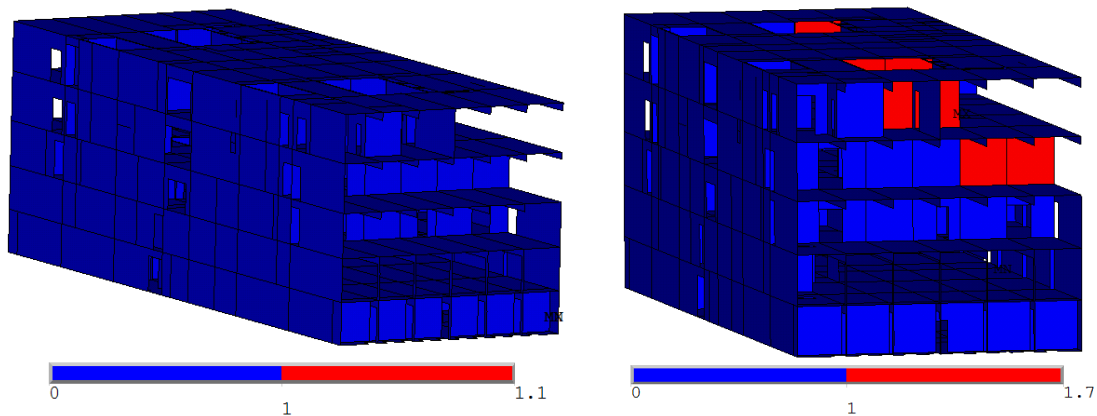


Figure 24 Plot of usage of the panels. Left - Initial case and right - structure at 4mm thickness

This assessment has been done considering the yield strength of the normal steel, including the Safety Factor, 180 N/mm^2 . Therefore, panels are exceeding by far the criteria, resulting in a need to change from steel grade A, to steel grade A36 for the panels subjected to analysis.

Table 10 Usage factor of panels for the initial case and the structure at 4mm thickness – Sagging bending moment

Initial Case				4mm Thickness			
Panel No.	von Mises [N/mm ²]	Mat_ID	Usage Factor	Panel No.	von Mises [N/mm ²]	Mat_ID	Usage Factor
140	146.8575	11	0.8159	140	305.5719	11	1.6976
150	134.7996	11	0.7489	150	263.4566	11	1.4636
166	120.3295	11	0.6685	166	247.5059	11	1.3750
136	118.9838	11	0.6610	136	245.3402	11	1.3630
218	107.6282	11	0.5979	218	166.8083	11	0.9267
151	104.5388	11	0.5808	151	203.3767	11	1.1299
135	104.1313	11	0.5785	135	221.4129	11	1.2301
160	101.378	11	0.5632	160	185.8419	11	1.0325
217	99.72547	11	0.5540	217	155.8054	11	0.8656
141	95.28325	11	0.5294	141	211.3334	11	1.1741

The next step is to implement the change of material for the failing panels, therefore these subjected to modification will receive a new type of material, respectively steel grade A36, considered high tensile steel in shipbuilding.

Table 11 Usage factors and new material ID after the material change – Sagging

4mm Thickness				Material Change			
Panel No.	von Mises [N/mm ²]	Mat_ID	Usage Factor	Panel No.	von Mises [N/mm ²]	Mat_ID	Usage Factor
140	305.5719	11	1.6976	140	305.5719	20	1.1193
150	263.4566	11	1.4636	150	263.4566	20	0.9650
166	247.5059	11	1.3750	166	247.5059	20	0.9066
136	245.3402	11	1.3630	136	245.3402	20	0.8987
218	166.8083	11	0.9267	218	166.8083	20	0.6110
151	203.3767	11	1.1299	151	203.3767	20	0.7450
135	221.4129	11	1.2301	135	221.4129	20	0.8110
160	185.8419	11	1.0325	160	185.8419	20	0.6807
217	155.8054	11	0.8656	217	155.8054	20	0.5707
141	211.3334	11	1.1741	141	211.3334	20	0.7741

The new material comes with a new identification number defined for the graphic representation, respectively 20, and will not affect the strength analysis performed by the software, but it will act as guidance to easier identify where the material has been relocated. Therefore, in Table 11, although the stress values are the same since ANSYS Mechanical does not consider the material strength for the computation, the usage factor is less in value, excepting one panel, whose stress still exceeds and this panel is subjected to fail yield in an extreme loading case. Although the usage factor is larger than 1, the stress is not higher than the yield strength of steel grade A36, which is $\sigma_y = 355 \text{ N/mm}^2$. This means the panel can withstand an additional 50 N/mm^2 without failing, but this is not a practice accepted by classification societies. In Figure 25, it is visible that the usage of the panels has been decreased considerably. The one panel with usage value higher than 1 it is not visible from the plot of the entire model, but the fact that all the other panels display a blue colour provides that the material is changed and assuming a higher stress criterion, respectively $\sigma_0^2 = 273 \text{ N/mm}^2$, the panels are strengthened against yield failure.

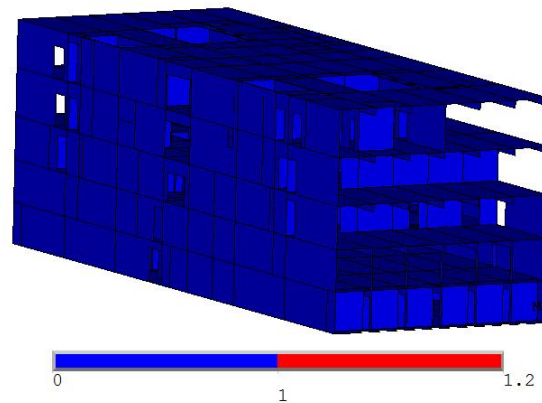


Figure 25 Usage factor distribution after the material change

Another factor to be considered is that the vessel is a very large and complex structure and for the current analysis only a section comprised of 440 panels is chosen, meaning that in a global investigation of the structural strength, these loads will distribute in a more even manner, giving better results.

Hogging

The hogging case is similar to the previous one where panels are investigated at their initial condition in the model provided by the company. After thorough strength analysis, the structure seems well-dimensioned, as only two panels have usage factors exceeding the value of 1, but by very less. Therefore, the first approach is to change the thickness uniformly to the lowest available thickness for the normal steel used in shipbuilding, respectively 4mm and perform new strength analysis. After these first steps, usage factors for the new initial case for the model are computed and the new usage values are analysed. In Figure 26, in the left structure, there is only one panel failing, respective to the initial loading case. In the right figure, the panels failing are larger in number, and we can recollect from the thickness changing optimization part that 41 panels were failing initially in the hogging case, at 4mm thickness uniformly distributed. This is visible by the many red panels.

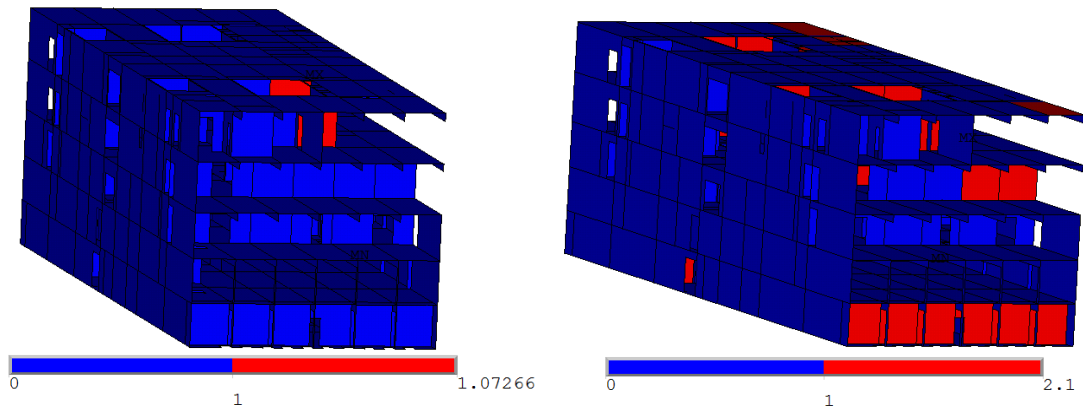


Figure 26 Plot of usage of the panels during hogging loading case. Left - Initial case and right - structure at 4mm thickness

This allows to implement the material change, which once again will not give different stress values in the strength analysis, but it will provide increased stress limit, keeping the material from failing under yield.

In Table 12 these facts are visible, as initially, the panels provide structural stability, and in the new case, they require optimization.

Table 12 Usage factor of panels for the initial case and the structure at 4mm thickness - Hogging

Initial Case				4mm Thickness			
Panel No.	von Mises [N/mm ²]	Mat_ID	Usage Factor	Panel No.	von Mises [N/mm ²]	Mat_ID	Usage Factor
150	193.0782	11	1.0727	150	355.2378	11	1.9735
140	187.3937	11	1.0411	140	377.2538	11	2.0959
151	178.9636	11	0.9942	151	307.582	11	1.7088
166	168.836	11	0.9380	166	329.7332	11	1.8319
160	138.8976	11	0.7717	160	236.9323	11	1.3163
141	136.5998	11	0.7589	141	286.4044	11	1.5911
436	132.4392	11	0.7358	436	235.8421	11	1.3102
152	130.3486	11	0.7242	152	215.8953	11	1.1994
167	121.5709	11	0.6754	167	250.1899	11	1.3899
162	118.5311	11	0.6585	162	192.8696	11	1.0715

For the optimization purpose, a new material ID is assigned, as described in the sagging case. Material with ID 20 is introduced as steel grade A36, with the yield criteria, including safety factor, of 273 N/mm². After having changed the material for all the panels having initially a usage factor of more than 1, a decrease in the values of the usage factors is observed. Some panels still exceed the imposed criteria, as seen in Figure 27, but if looking closely to the real yield strength of the steel grade A36, which is $\sigma_{y2} = 355 \text{ N/mm}^2$, some panels can still

withstand excessive loads up to some extent, and for those exceeding the yield strength of the material without having considering any safety factor, additional strengthening measures will be imposed.

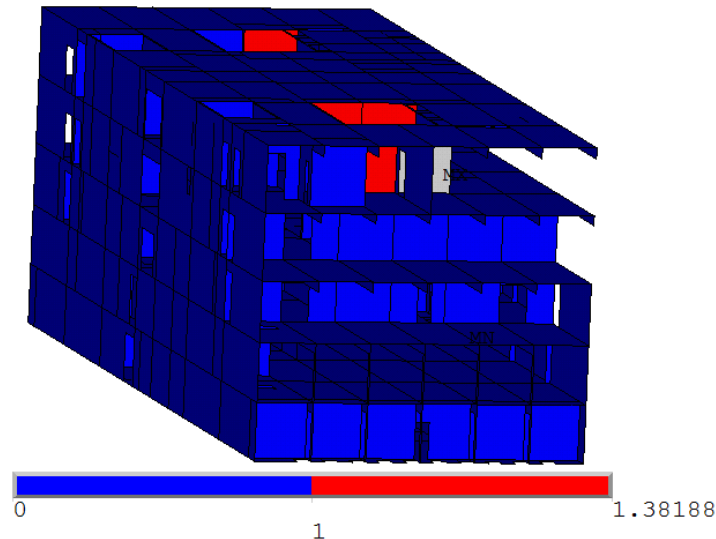


Figure 27 Usage factor distribution after the material change

Table 13 Usage factors and new material ID after the material change - Hogging

4mm Thickness				Material Change			
Panel No.	von Mises [N/mm ²]	Mat_ID	Usage Factor	Panel No.	von Mises [N/mm ²]	Mat_ID	Usage Factor
150	355.2378	11	1.9735	150	355.2378	20	1.3012
140	377.2538	11	2.0959	140	377.2538	20	1.3819
151	307.582	11	1.7088	151	307.582	20	1.1267
166	329.7332	11	1.8319	166	329.7332	20	1.2078
160	236.9323	11	1.3163	160	236.9323	20	0.8679
141	286.4044	11	1.5911	141	286.4044	20	1.0491
436	235.8421	11	1.3102	436	235.8421	20	0.8639
152	215.8953	11	1.1994	152	215.8953	20	0.7908
167	250.1899	11	1.3899	167	250.1899	20	0.9164
162	192.8696	11	1.0715	162	192.8696	20	0.7065

4.3 Results

In this paper the focus is on the average stress levels per panel, to simplify the problem and have a more realistic view of the values of the constraints. This means that assessing the structural analysis with the finite element method would provide nodal and elemental solutions.

Since a cruise vessel is a very large and complex structure, the focus is not on the elemental stress values, but on the average, that occurs in each panel. This gives a more practical approach for a shipyard, where if needed, panels failing their material limit can be replaced by either panel with a material having a higher limit, or panels of larger thickness.

4.3.1 Sagging

In the following figures, the nodal stress values of the equivalent von Mises are plotted. To avoid uncertainties, the scales are not displayed, as the plotting of the stresses is done per nodal solution and not by panel, as the values shown in tables in the sections above.

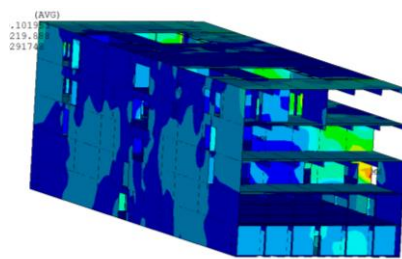


Figure 28 Nodal stress assessment - Initial case

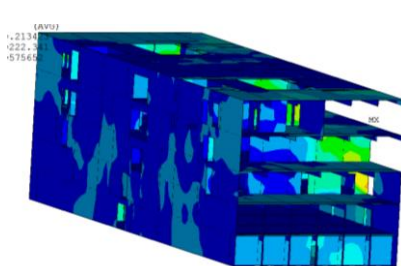


Figure 29 Nodal stress assessment - structure at 4mm thickness

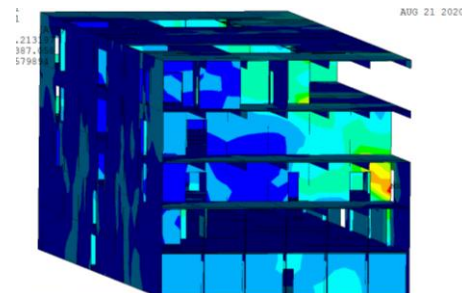


Figure 30 Nodal stress assessment - Optimized structure

The three images are plotted consequently, after having modified the structure. The first, on the left side, displays the stress distribution in the initial structure, with no modification, but only having loaded the sagging bending moment and respective boundary conditions. The second is the structure after having uniformly changed the thicknesses of all panels to 4mm. It is noted that the left extremity, depicting one of the transverse bulkheads, has a larger distribution of lower stress values (in dark blue colour), therefore the larger stresses are concentrated on the right side of the structure, as seen in the section previous described, where for the sagging case, the panels exceeding the yield criteria are situated on the right half of the model. The third image, which represents the distribution of stresses after the end of the

optimization shows that there is a small stress concentration in one of the panels, keeping nodal stress at high values. This is due to the large stress in two of the elements, followed by lower stresses adjacent elements. This is shown in the figure below, where a zoom of the situation is presented, in a plot of the elemental stress distribution. In Figure 32 it is visible that the value of the elements giving high stresses is situated in the range of 519 N/mm², and some of the adjacent panels have stress values of 200 N/mm² less. This can lead to localized higher stress areas due to the discontinuity in thickness between the panels.

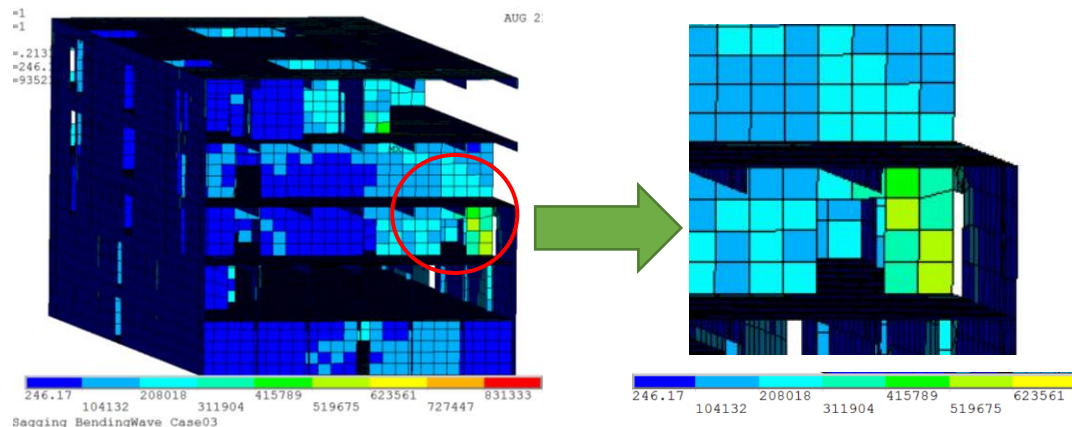


Figure 31 Elemental stress distribution of optimized structure - Sagging

Figure 32 Zoom over Figure 31

In Figure 33, a graph showing the evolution of the optimization is displayed, where in the sagging bending wave condition, as mentioned in section 4.1.1, eight panels initially fail by yielding having average equivalent stress values larger than the 180 N/mm² criteria. The criteria mentioned before represents one of the optimization constraints, as explained in the theoretical chapter of the thesis. Therefore, on the vertical axis, the number of panels failed is represented, with circular points showing the number of panels that fail by yielding at each iteration. It took six iterations to optimize the structure, representing a shorter optimization loop than in the hogging case.

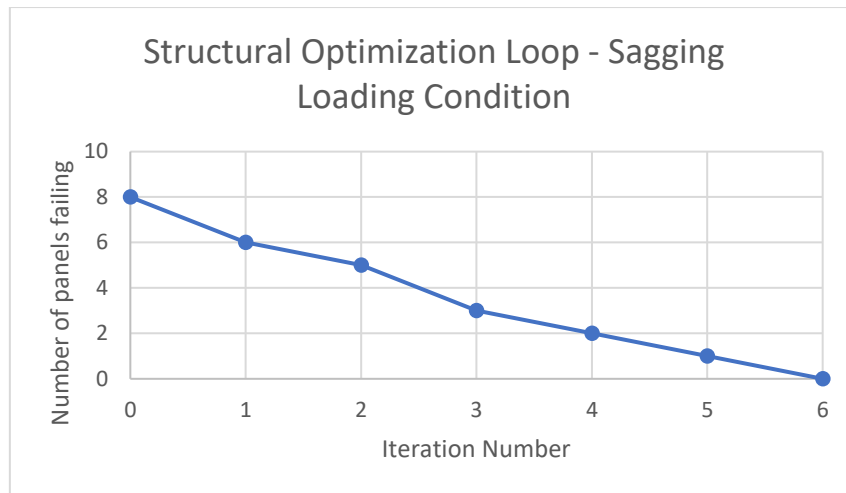


Figure 33 Optimization loop for the sagging loading condition

In Figure 35, an estimative cost of the material of the structure is assessed, by giving an insight over the cost of production, disregarding labour costs, such as welding costs, which can affect highly the value of the vessel. For this assessment, two materials are considered, steel grade A and steel grade A36, where the first has a price of 800 €/ton and the second has a price of 815 €/ton (the prices are informative and they can vary based on the market speculations).

Therefore, by starting the optimization with a new initial case, where the structure has a uniformly distributed 4mm thickness, the mass increase with the thickness change is observed in Figure 34, where the increase is steady up to the optimization point. The respective cost of the structure is calculated upon size optimization and it gives a total increase of 0.98% after considering the new initial case of the structure.

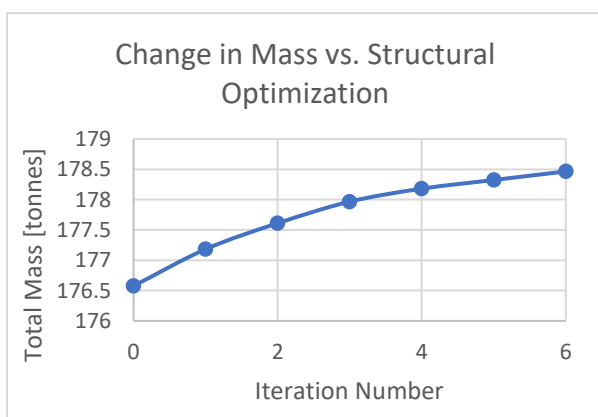


Figure 34 Mass behaviour proportional to the size optimization

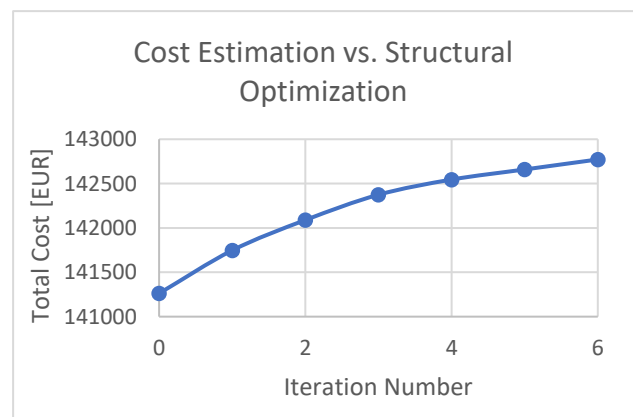


Figure 35 Cost estimation of the structure after size optimization

Based on the two graphs, the shape of the curve follows the same path, meaning that the cost is increasing proportionally to the increase in mass and the mass increases by adding more thickness to the panels, outcome which does not come as a surprise as by adding thickness the mass increases and the cost of the material is increased as the tonnage is higher. The mass increase of only 0.98% does not represent a large cost addition to the production costs. It is a cost that can be insured by the better structural strength provided upon the optimization process.

The cost estimation presented above is in the case of optimizing the structure by modifying the panels' thickness. When optimizing the structure by changing the material, the mass will not change, as the thickness will be the same for the second material, but as mentioned previously, the stress limit is increased, allowing the panels to withstand more loads. Therefore, the estimative cost difference for the case when the panels failing have their material changed to steel grade A is shown in Figure 36. Here an increase of 0.98% in cost has occurred. Although the mass of the structure is the same, the price per ton differs from one material to the other, therefore the growth in cost is linear, assessed in one iteration.

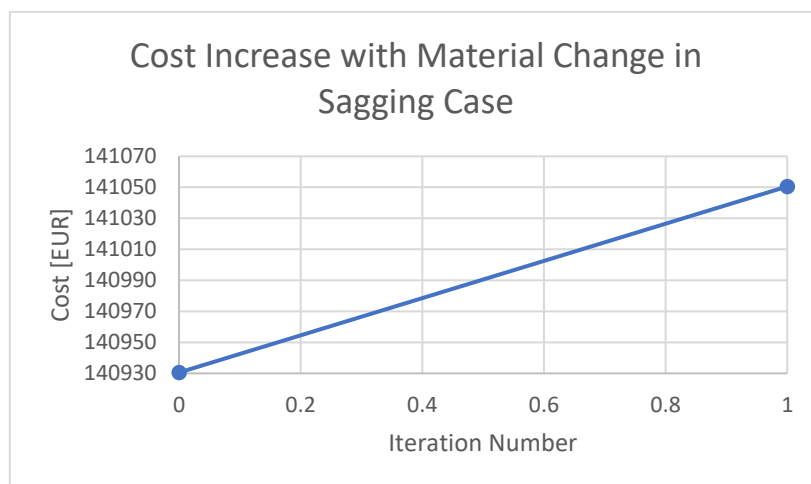


Figure 36 Cost Increase for Material Change – Sagging

4.3.2 Hogging

The structure is now subjected to hogging loading condition, respectively the midship section is situated on a crest. The optimization algorithm has been followed and the same procedure has been used as in the sagging loading case, considering the stress limit of $\sigma_0^1 = 180 \text{ N/mm}^2$.

In this case, the magnitude of the stresses is larger than the previous situation, giving a starting of 41 panels yielding. After having applied thickness increase, the number of panels failing has

dropped by 36.5%, leaving 26 panels to be optimized after the first iteration. This process follows until the structure reaches optimum values of stresses, not exceeding the yield criteria. There are parts in the optimization process where it displays a plateau, due to several panels having larger stresses than the others and due to the large discrepancy in thicknesses between some of the panels, the stresses take more iterations to achieve lower values than 180 N/mm^2 . This phenomenon takes place because there are panels that have stresses in the normal range, but as mentioned, a non-uniform thickness distribution leads to localized stresses. These require strengthening; therefore, the thickness is being increased, but the total number of panels still to be optimized does not change.

It is visible in Figure 37 that the optimization process for the hogging case is lengthy and it is also time-consuming, requiring more iterations. In the following figures, Figure 38 and Figure 39 the mass increase and the respective cost estimation are shown, where the graphs follow the same path as in the sagging case, where the cost is proportional to the mass modification. Whether the mass decreases, the cost will also decrease as it is dependant on the mass fluctuation in the structure.

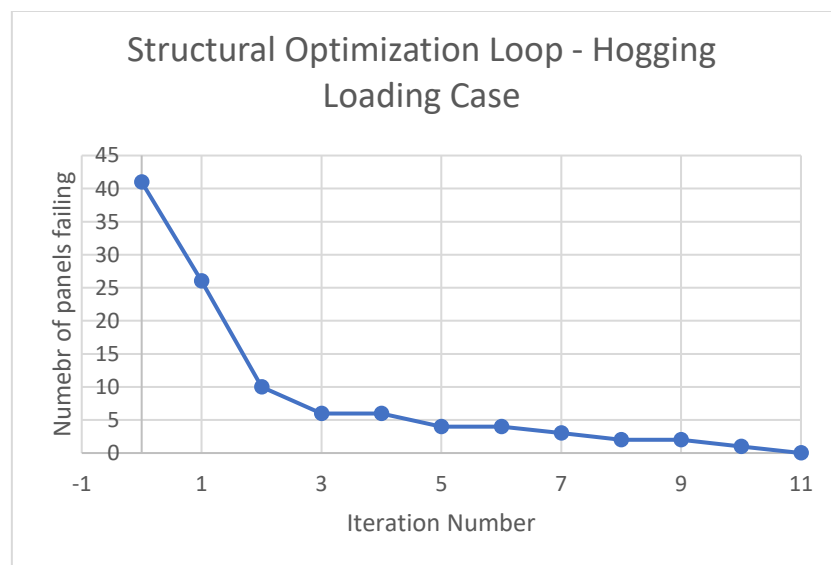


Figure 37 Optimization loop for the hogging loading condition

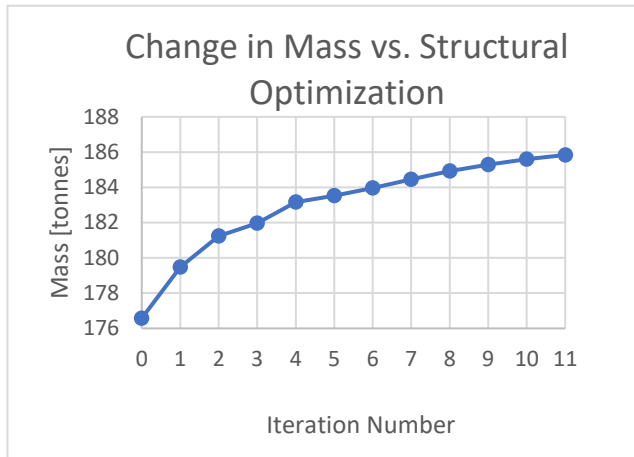


Figure 38 Mass behaviour with respect to size optimization

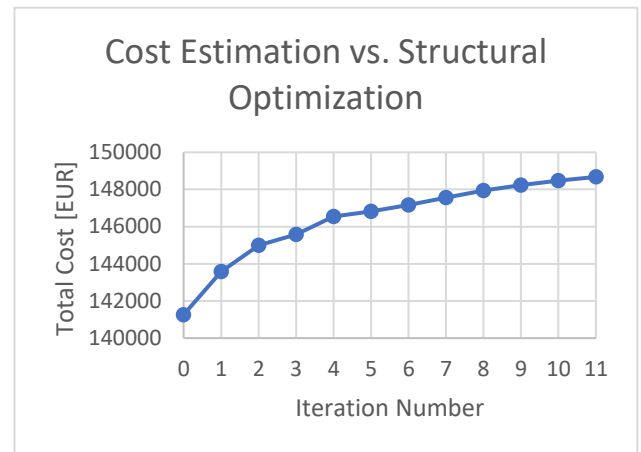


Figure 39 Cost estimation of the structure after size optimization

With a different optimization approach, Figure 40 shows the difference of cost (estimation) after having changed the material grade of the 41 panels yielding at the beginning. As explained previously, the hogging loading case provides higher stresses in the structure due to the loads and boundary conditions that are applied to the vessel. After the modification, there is a slight increase in the cost of the model, by 1.2%. Still, the mass of the structure does not increase as the thickness of the panels is considered the same, the only parameter changing is the material property, from the normal steel to higher tensile steel.

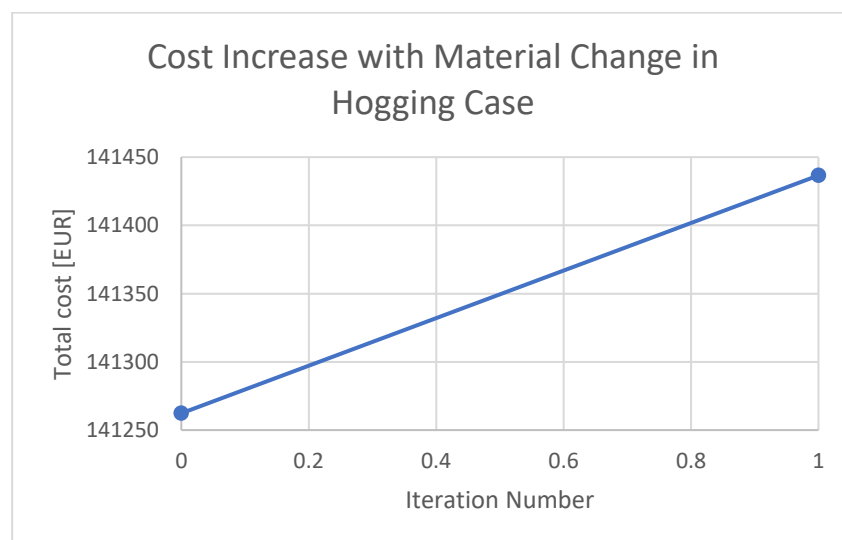


Figure 40 Cost Increase for Material Change - Hogging

Nevertheless, different approaches can be considered for the optimization process of such complex structures. In this case, to achieve lower stresses than the imposed criteria, the process has become too long. In real life, a more practical approach can be assumed, such as changing the material for more panels than the targeted number of failing members to provide uniform strength of areas of the structure with larger stress concentrations.

5 CONCLUSION

In this study, the main focus is on the study of the yield strength of a cruise vessel and the possible and feasible structural optimization methods that can be implemented to provide structural integrity along with focus on optimizing the objective functions considering the imposed constraints. The main constraints have been technological, respectively the thickness available for normal and high tensile steel that can be used in shipyards. Another constraint has been the fixed geometry of the structure. These two main criteria have sculpted the idea of size (scantling) optimization. An additional optimization method used was the change of material grade, which is a practice commonly used in shipyards that have the infrastructure for such implementation.

For this project, the structural optimization methods were implemented by trial and error simulations in ANSYS Mechanical. To ease the implementation of the optimization path, algorithm codes have been written to build an automatized optimization process.

In assessing the structural optimization of a cruise vessel, safety structural requirements are to be considered. Therefore, partial safety factors have been assigned to the yield strength criterion used for the assessment of the structural stresses. These were calculated based on DNV-GL rules.

The objective of the optimization is to reduce structural weight and provide lower costs for the production process and the operation of the vessel. In this thesis, the approach was to provide an optimized structure that can withstand loads within the yield criterion.

For the size optimization, the model subjected to analysis has been analyzed within 6, respectively 11 iterations for the two different loading cases. Upon the optimization algorithm, we can observe a decrease of the stresses that occur in the structure. In some parts of the model local maximum stresses still exist, but this has due to the boundary conditions and loads applied to the local and global structure and the discrepancies in thicknesses between panels. This was also influenced the fact that the structure provided by the company was well-dimensioned and the stresses occurring were not exceeding the yield criteria, which led to a uniform change of thickness to 4mm, respectively the minimum allowed thickness for the normal steel used in shipbuilding. Later in the optimization algorithm, panels that have reached thicknesses two times larger than the initial panel thickness, or have exceeded that value, have shown local maximum in terms of equivalent von Mises stresses. An approach to minimize the occurrence

of having this phenomenon is to perform more optimization loops until the perfect case has been found, respectively a more uniform distribution of the thickness, respecting the technological limits presented in the theoretical part of this thesis.

For a more practical approach, the change of material to a better strength one was considered and based on the same yield criteria assumption, the usage factors of each panel have been computed. The values exceeding unity represented the panels failing by yield. Therefore, for these panels, the material has been changed from steel grade A as normal shipbuilding steel to steel grade A36 as high tensile steel that provides a larger stress capacity, respectively more structural strength, and new usage factors have been calculated, showing that depending on the loading condition, some panels are more influenced by others, having larger utility even after changing the material. This optimization method shows that the stresses in the panels do not change, since the boundary conditions and loads are the same, distributed within the same dimensioned panel having the same thickness. The only change is the allowable stress limit provided by the new material.

In the size optimization case, the process is lengthy and requires high computational resources and time. Nevertheless, the iterative steps can be stopped when the panels' stresses are between the yield criterion that includes the safety factor and the actual material yield strength. In that range the panels have structural strength provided by the material properties and additional strengthening measures can be considered such as redistribution of thickness in adjacent panels, re-dimensioning of structural stiffening members such as girder, longitudinals and frames, if possible, with consideration of the imposed constraints.

The material changing has provided to be a shorter and more efficient method, where compared to size optimization, the structural mass does not increase drastically as the densities of the two materials are considered equal for this analysis since the thickness is kept the same. This process is easier to implement within a shipyard as changing the material, does not require additional welding techniques like the changing of thickness. Also, the price per ton of the types of material does not differentiate by much, hence the new material would provide more strength by keeping the production costs nearly similar. There are challenges met in this process also, as some panels will still yield under the considered loads, and for this additional stiffening can be considered, as mentioned in the previous case. If panels have different thicknesses, the accumulation of stresses can be avoided by changing the thickness of adjacent panels, providing a more uniform weld, respectively reducing welding stress concentrations.

In conclusion, the structural optimization analysis has been performed on a smaller sized model at the midship, as at this location stresses are higher, to maintain a shorter computational time and to assess the structural behaviour. Also, by providing changes in the smaller model, the entire vessel will be influenced, and the overall stresses change according to the local structural assessment. On the other way around, by modifying properties on a larger scale, the local member will suffer modifications.

The optimization is, therefore, more efficient by considering the change in material grade first, and the change in thickness secondly, after defining which panels require additional strengthening measures.

6 FURTHER WORK

Possible further work that can be carried for the enrichment of this thesis is:

- Combination of both size optimization and material change in order to reach the output in shorter iterative steps.
- Strength analysis considering a larger part of the vessel which can give a better insight on the behaviour of the decks in the superstructure.
- Scantling optimization can be carried out in a more extensive way, taking into account the stiffeners, their dimensions and the spacing between them.
- Improvement of the optimization algorithm to consider more complex structural elements, such as curved side shells, curved panels, panels consisting of both longitudinal and transverse stiffening.
- Welding considerations could be included in the cost estimation to provide a more accurate production cost.
- Consideration of optimization algorithm that can incorporate yielding, buckling and deflection of the structure.

7 ACKNOWLEDGMENTS

I extend my gratitude to my supervisors Michael Zimmermann and Dipl. Ing Stefan Griesch from MV WERFTEN shipyard for making this opportunity possible for me to carry out my master's thesis. I also express my appreciation for their assistance and supervision during the course of this thesis and in making this work a success.

My special acknowledgement goes to Professor Patrick Kaeding and Thomas Lindemann for being there to guide and provide assistance to me during this academic trajectory. I learnt a lot during this short time with you and I express my respect and gratitude for feeding in me both academic and professional knowledge which will be of benefit in my future pursuit.

I also would love to thank Professor Rigo, Christine Reynders, and all the coordinators of the EMship+ M120 program inclusive of all the professors who have been part of this program. Thank you for the knowledge and experience shared during this academic path.

I express my special appreciation to my course mates Midhun Kanadan, Umunnakwe Chisom Bernard, and Andre Paiva who have had the patience in assisting me in one way or the other and were always ready to help during the course of this master's program. I sincerely express my appreciation to you all, and I wish us the best in the future ahead.

Finally, I thank my family and relatives for being there for me and assisting me in both thick and thin. You have shown me motivation and love and I extend my warm admiration. I am glad to share with you in the joy of this new academic achievement.

Daniela Laura Lungu

8 REFERENCES

- Ansys®. (n.d.). Ansys® Academic Research Mechanical and CFD, Release 18.2.
- BEAM 188*. (n.d.). Retrieved from https://www.mm.bme.hu/~gyebro/files/ans_help_v182/ans_elem/Hlp_E_BEAM188.html
- Bendsoe, M. P., & Sigmund, O. (2003). *Topology Optimization: theory, methods, and applications*. Berlin, Germany: Springer.
- Caendkoelsch. (2018, June 9). *What is the difference between essential and natural boundary conditions in FEM?* Retrieved from Caendkoelsch - A blog for FEM enthusiasts: <https://caendkoelsch.wordpress.com/2018/06/09/what-is-the-difference-between-essential-and-natural-boundary-conditions-in-fem/>
- Daley, C. (n.d.). *Ship Structures I*. St. John's, St. John's, Canada: Faculty of Engineering and Applied Sciences Memorial University.
- DNV. (2016). Hull structural design - Ships with length 100 metres and above. In DNV, *Rules from Classification of Ships* (p. 179).
- DNV A36 steel plate*. (n.d.). Retrieved from Shanghai Katalor Enterprises: [http://www.ice-steels.com/shipbuilding-steel/DNV-AH36-steel-plate.html#:~:text=DNV%20AH36%20steel%20is%20a%20kind%20of%20high%20tensile%20strength%20marine%20steel.&text=Higher%2Dstrength%20DNV%20shipbuilding%20steel,\(490%2D620%20MPa\)](http://www.ice-steels.com/shipbuilding-steel/DNV-AH36-steel-plate.html#:~:text=DNV%20AH36%20steel%20is%20a%20kind%20of%20high%20tensile%20strength%20marine%20steel.&text=Higher%2Dstrength%20DNV%20shipbuilding%20steel,(490%2D620%20MPa)).
- DNV Grade A shipbuilding steel plate*. (n.d.). Retrieved from Shanghai Katalor Enterprises: [http://www.ice-steels.com/shipbuilding-steel/DNV-Grade-A-shipbuilding-steel-plate.html#:~:text=The%20DNV%20A%20grade%20steel,Det%20Norske%20Veritas%20\(DNV\)](http://www.ice-steels.com/shipbuilding-steel/DNV-Grade-A-shipbuilding-steel-plate.html#:~:text=The%20DNV%20A%20grade%20steel,Det%20Norske%20Veritas%20(DNV))).
- DNV-GL. (2015). Part 5 Ship Types Chapter 5 Passenger Vessels. In DNV-GL, *Rules for Classification* (p. 25).
- DNV-GL. (2015). Part 5 Ship types, Chapter 4 Passenger ships. In *Rules for Classification*.
- DNV-GL. (2017). Part 3 Hull, Chapter 4 Loads. In *Rules for Classification*.
- Elasticity (physics)*. (n.d.). Retrieved from Wikipedia: [https://en.wikipedia.org/wiki/Elasticity_\(physics\)#:~:text=The%20physical%20reasons%20for%20elastic,is%20added%20to%20the%20system\).&text=The%20material's%20elastic%20limit%2C%20the,the%20onset%20of%20permanent%20deformation](https://en.wikipedia.org/wiki/Elasticity_(physics)#:~:text=The%20physical%20reasons%20for%20elastic,is%20added%20to%20the%20system).&text=The%20material's%20elastic%20limit%2C%20the,the%20onset%20of%20permanent%20deformation).
- Grade A shipbuilding steel plate*. (n.d.). Retrieved from BBN: <https://www.shipbuilding-steel.com/Products/A.html#:~:text=Grade%20A%20steel%20plate%20is,processing%20properties%2Cand%20welding%20properties>.
- Haftka, R. T., & Sobieszczanski-Sobieski, J. (2009). *Structural Optimization: History*. Retrieved from SpringerLink: https://doi.org/10.1007/978-0-387-74759-0_669
- Hughes, O. F. (1998). *Ship Structural Design: A Rationally-Based, Computer-Aided, Optimization Approach*. Jersey City, NJ: SNAME.

- Introduction to structural integrity.* (n.d.). Retrieved from The Open University:
<https://www.open.edu/openlearn/ocw/mod/oucontent/view.php?id=3459&printable=1#:~:text=Structural%20integrity%20is%20the%20study,into%20the%20engineering%20design%20process.>
- Kim, S. (2018, May 3). *13 things you didn't know about cruise ship design.* Retrieved from The Telegraph: <https://www.telegraph.co.uk/travel/cruises/articles/cruise-ship-design-things-you-didnt-know/#:~:text=%E2%80%9CA%20cruise%20ship's%20structural%20grid,the%20director%20of%20WKK%20Architects.&text=%E2%80%9CCruise%20ships%20are%20like%20giant%20floating%20t>
- Lazakis, I., & Turan, O. (2009). The effect of increasing the thickness of the ship's structural members on the Generalised Life Cycle Maintenance Cost (GLCMC). *Proceedings of IMPROVE Final Workshop*, (pp. 61-67). Dubrovnik, Croatia.
- Lindemann, T., & Kaeding, P. (2010). An Approach to Optimization in Ship Structural Design Using Finite Element and Optimization Techniques. *Proceedings of the Twentieth (2010) International Offshore and Polar Engineering Conference* (pp. 803-808). Beijing, China: The International Society of Offshore and Polar Engineers (ISOPE).
- Longitudinal Strength of Ships – Hogging and Sagging Moment.* (2019, March 12). Retrieved from World Maritime Affairs: <https://www.worldmaritimeaffairs.com/longitudinal-strength-of-ships-hogging-and-sagging-moment/>
- Mansour, A., & Liu, D. (2008). *The Principles of Naval Architecture Series*. Jersey City, NJ: SNAME.
- Matmatch. (2020). *Yield Strength vs. Tensile Strength - What's the Difference?* Retrieved from Matmatch: <https://matmatch.com/learn/property/difference-between-yield-strength-tensile-strength>
- Menon, A. (2020, 06 26). *Understanding Draft Surveys – Importance, Calculations & Errors.* Retrieved from Marine Insight: <https://www.marineinsight.com/naval-architecture/draft-surveys-calculations-errors/>
- MV WERFTEN Wismar, G. (n.d.). *Giants Made in MV - The Global Class.* Retrieved from MV Werften: <https://www.mv-werften.com/de/schiffe/global.html>
- Paik, J. K., & Kim, B. J. (2002). Ultimate strength formulations for stiffened. *Thin-Walled Structures* 40, 45-83.
- Rigo, P. (2001). A module-oriented tool for optimum design of stiffened structures - Part I. *Marine Structures* 14 , 611- 629.
- Rigo, P., & Rizzuto, E. (2003). Analysis and Design of Ship Structure. In I. G. Authorities, *Ship Design and Construction* (pp. 18-1 - 18-77). Jersey City, NJ: The Society of Naval Architects and Marine Engineers.
- Sekulski, Z. (2009). Structural weight minimization of high speed. *Polish Maritime Research* 2(60), 11-23.
- SHELL 181.* (n.d.). Retrieved from https://www.mm.bme.hu/~gyebro/files/ans_help_v182/ans_elem/Hlp_E_SHELL181.html

- Sparta. (n.d.). *Static Loading - Sparta Engineering*. Retrieved from Sparta Designing Solutions:
<https://www.spartaengineering.com/glossary/static-loading/#:~:text=Static%20loading%20is%20a%20load,on%20them%20then%20dynamic%20loading.>
- Stolarski, T., Nakasone, Y., & Yoshimoto, S. (2006). *Engineering Analysis with ANSYS Software*.
- Svanberg, K. (n.d.). *Structural Optimization*. Retrieved from
<https://www.math.kth.se/optsys/Struc.html#:~:text=Structural%20optimization%20is%20a%20discipline,of%20load%2Dcarrying%20mechanical%20structures.>
- Thompson, M. K., & Thompson, J. M. (2017). *ANSYS Mechanical APDL for Finite Element Analysis*.
- UNICAMP. (n.d.). APDL Basics. 1-16. Campinas, Sao Paulo, Brazil.
- USNA. (n.d.). *EN200 Naval Engineering I*. Retrieved from United States naval Academy:
https://www.usna.edu/NAOE/_files/documents/Courses/EN400/02.06%20Chapter%206.pdf
- Wikipedia Foundation, I. (2019). *Pure Bending*. Retrieved from Wikipedia The Free Encyclopedia:
https://en.wikipedia.org/wiki/Pure_bending
- Yu, Y. Y., Jin, C. G., Lin, Y., & Ji, Z. S. (2010). A practical method for ship structural optimization. *Proceedings of the Twentieth (2010) International Offshore and Polar Engineering Conference* (pp. 797-802). Beijing, China: The International Society of Offshore and Polar Engineers (ISOPE).

APPENDIX A - Results of size optimization – Sagging loading condition

Table 14 First Iteration – size optimization

First Iteration							
Panel No.	von Mises [N/mm ²]	Section ID	Thickness [mm]	Panel No.	von Mises [N/mm ²]	Section ID	Thickness [mm]
140	305.5719	10009	4	140	273.1813	10010	5
150	263.4566	10009	4	150	231.9858	10010	5
166	247.5059	10009	4	166	217.5648	10010	5
151	245.3402	10009	4	151	224.913	10010	5
141	166.8083	10009	4	141	165.3125	10009	4
167	203.3767	10009	4	167	176.0082	10010	5
160	221.4129	10009	4	160	199.307	10010	5
436	185.8419	10009	4	436	163.4123	10010	5
169	155.8054	10009	4	169	154.6265	10009	4
168	211.3334	10009	4	168	185.6509	10010	5

Table 15 Second Iteration - size optimization

Second Iteration							
Panel No.	von Mises [N/mm ²]	Section ID	Thickness [mm]	Panel No.	von Mises [N/mm ²]	Section ID	Thickness [mm]
140	273.1813	10010	5	140	245.59	10011	6
150	231.9858	10010	5	150	206.8651	10011	6
166	217.5648	10010	5	166	195.0074	10011	6
151	224.913	10010	5	151	208.6483	10011	6
141	165.3125	10009	4	141	164.841	10009	4
167	176.0082	10010	5	167	174.3732	10010	5
160	199.307	10010	5	160	181.9105	10011	6
436	163.4123	10010	5	436	162.7145	10010	5
169	154.6265	10009	4	169	153.9844	10009	4
168	185.6509	10010	5	168	166.5139	10011	6

Table 16 Third Iteration - size optimization

Third Iteration							
Panel No.	von Mises [N/mm ²]	Section ID	Thickness [mm]	Panel No.	von Mises [N/mm ²]	Section ID	Thickness [mm]
140	245.59	10011	6	140	222.5045	10012	7
150	206.8651	10011	6	150	187.2602	10012	7
166	195.0074	10011	6	166	177.0097	10012	7
151	208.6483	10011	6	151	194.75	10012	7
141	164.841	10009	4	141	164.4664	10009	4
167	174.3732	10010	5	167	173.2632	10010	5

160	181.9105	10011	6	160	167.4543	10012	7
436	162.7145	10010	5	436	162.1767	10010	5
169	153.9844	10009	4	169	153.4946	10009	4
168	166.5139	10011	6	168	166.9221	10011	6

Table 17 Fourth Iteration - size optimization

Fourth Iteration							
Panel No.	von Mises [N/mm ²]	Section ID	Thickness [mm]	Panel No.	von Mises [N/mm ²]	Section ID	Thickness [mm]
140	222.5045	10012	7	140	203.1466	10013	8
150	187.2602	10012	7	150	171.3326	10013	8
166	177.0097	10012	7	166	176.9106	10012	7
151	194.75	10012	7	151	181.2574	10013	8
141	164.4664	10009	4	141	164.3038	10009	4
167	173.2632	10010	5	167	172.382	10010	5
160	167.4543	10012	7	160	170.1397	10012	7
436	162.1767	10010	5	436	161.9982	10010	5
169	153.4946	10009	4	169	153.4179	10009	4
168	166.9221	10011	6	168	166.9618	10011	6

Table 18 Fifth Iteration - size optimization

Fifth Iteration							
Panel No.	von Mises [N/mm ²]	Section ID	Thickness [mm]	Panel No.	von Mises [N/mm ²]	Section ID	Thickness [mm]
140	203.1466	10013	8	140	186.6917	10014	9
150	171.3326	10013	8	150	170.8647	10013	8
166	176.9106	10012	7	166	176.8681	10012	7
151	181.2574	10013	8	151	170.1166	10014	9
141	164.3038	10009	4	141	164.2313	10009	4
167	172.382	10010	5	167	172.0224	10010	5
160	170.1397	10012	7	160	172.5315	10012	7
436	161.9982	10010	5	436	161.9142	10010	5
169	153.4179	10009	4	169	153.3732	10009	4
168	166.9618	10011	6	168	167.2796	10011	6

Table 19 Sixth Iteration - size optimization

Sixth Iteration							
Panel No.	von Mises [N/mm ²]	Section ID	Thickness [mm]	Panel No.	von Mises [N/mm ²]	Section ID	Thickness [mm]
140	186.6917	10014	9	140	178.664	10015	10
150	170.8647	10013	8	150	170.8606	10013	8
166	176.8681	10012	7	166	176.8679	10012	7

151	170.1166	10014	9	151	170.1171	10014	9
141	164.2313	10009	4	141	164.2303	10009	4
167	172.0224	10010	5	167	172.0231	10010	5
160	172.5315	10012	7	160	172.5314	10012	7
436	161.9142	10010	5	436	161.9088	10010	5
169	153.3732	10009	4	169	153.3616	10009	4
168	167.2796	10011	6	168	167.28	10011	6